Journal of Molecular Structure 1244 (2021) 130976

Contents lists available at ScienceDirect

Journal of Molecular Structure

journal homepage: www.elsevier.com/locate/molstr

Effect of hydrocarbon chain length for acid corrosion inhibition of mild steel by three 8-(n-bromo-R-alkoxy)quinoline derivatives: Experimental and theoretical investigations

A. Tazouti[a], N. Errahmany[a], M. Rbaa[b], M. Galai[a], Z. Rouifi[b], R. Touir[a,c,*], A. Zarrouk[d], S. Kaya[e], M. Ebn Touhami[a], B. El Ibrahimi[f], S. Erkan[g]

[a] Advanced Materials and Process Engineering Laboratory, Faculty of Science, Ibn Tofail University, Kenitra, Morocco
[b] Laboratory of Agro-Resources, Polymers and Process Engineering, Department of Chemistry, Faculty of Sciences, Ibn Tofail University, P.O. Box 242, 14000, Kenitra, Morocco
[c] Regional Center for Education and Training Professions (CRMEF), Kenitra, Morocco
[d] Laboratory of Materials, Nanotechnology and Environment, Faculty of Sciences, Mohammed V University, Av. Ibn Battouta, P.O. Box. 1014, Agdal-Rabat, Morocco
[e] Sivas Cumhuriyet University, Health Services Vocational School, Department of Pharmacy, 58140, Sivas, Turkey
[f] Team of Physical Chemistry and Environment, Faculty of Sciences, Ibn Zohr University, 80000 Agadir, Morocco
[g] Sivas Cumhuriyet University, Faculty of Science, Department of Chemistry, 58140, Sivas, Turkey

ARTICLE INFO

Article history:
Received 6 May 2021
Revised 22 June 2021
Accepted 23 June 2021
Available online 27 June 2021

Keywords:
Length of the hydrocarbon chain effect
8-(n-bromo-R-alkoxy)quinoline derivatives
Corrosion inhibition
Electrochemical measurements
Theoretical investigations

ABSTRACT

Three 8-(n-bromo-R-alkoxy) quinoline derivatives with a length of the hydrocarbon chain, namely 8-(2-bromoethoxy) quinoline (QN-C2Br), 8-(3-bromopropoxy) quinoline (QN-C3Br) and 8-(4-bromobutoxy) quinoline (QN-C4Br) were prepared and characterized by proton and carbon NMR spectroscopy (1H NMR and 13C NMR). Thus, to evaluate the effect of these compounds on the mild steel (MS) corrosion inhibition in 1.0 M HCl, electrochemical methods of potentiodynamic polarization curves and electrochemical impedance spectroscopy were used. The potentiodynamic polarization curves showed that the tested products act as an anodic - type inhibitor. Thus, EIS designated that the charge transfer resistance arises from 32.41 Ω cm2 to 705.21 Ω cm2, 783.21 Ω cm2 and 1389.12 Ω cm2 at 10−3 M of QN-C2Br, QN-C3Br and QN-C4Br, respectively. In addition, it is found that the adsorption of three compounds on the MS surface obeys the Langmuir adsorption isotherm equation. It is found also that these products take their inhibition efficiency at high temperature. SEM analysis of the surface and UV-visible spectroscopy of the solution indicates the formation of a protective layer on MS surface and an inhibitor-complex in solution, respectively. Finally, to understand the adsorption properties of the studied 8-(n-bromo-R-alkoxy)quinolone derivatives, density functional theory (DFT) calculations and molecular dynamics (MD) simulation were achieved. These theoretical studies indicated that the anti-corrosion performance of the tested molecules follows the trend: QN-C4Br > QN-C3Br > QN-C2Br. This trend is very compatible with the experimental results.

1. Introduction

Corrosion is considered one of the pivotal problems of the world industry, which gravely destroys industrial and natural environments. Today, it is mostly recognized that corrosion is a harmful process for the environment and the economy [1,2]. It is known that iron and its alloy are widely used in various industries. One of their shortcomings is subject to corrosion in different industrial operating media, especially in acidic solutions [3], like as industrial pickling and cleaning baths [4]. To avoid this unwelcome problem, many organic inhibitors are frequently used [5]. Their selection depends on the acid type, their concentrations, the temperature solution and chemical composition of the metals [6]. Thus, perusal of literature reveals that the inhibitors contain -S atoms in their molecular structure are effective in sulphuric acid, while those contain -N atoms are effective in hydrochloric acid [7]. However, 8-hydroxyquinoline derivatives are good inhibitors for MS corrosion in acidic environments [8-10]. To achieve this, today's researchers are aiming to synthesize new 8-hydroxyquinoline compounds. Therefore, the majority of the employed inhibitors are

* Corresponding author.
E-mail address: touir8@yahoo.fr (R. Touir).

https://doi.org/10.1016/j.molstruc.2021.130976
0022-2860/

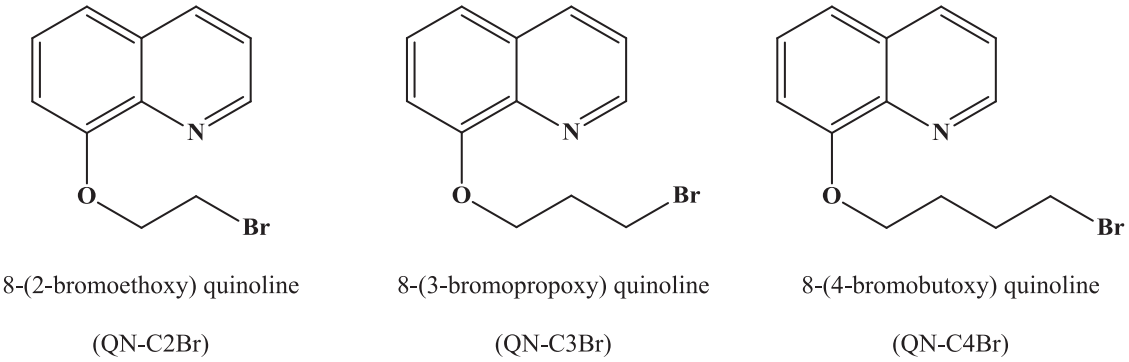

Fig. 1. Molecular structure of QN-C2Br, QN-C3Br and QN-C4Br.

organic compounds having hetero-atoms, like as oxygen, nitrogen and/or sulfur atoms, and double or multiple bonds, allowing adsorption on the metallic surface [11-14]. In addition, the effect study of some organic compounds containing bromide in their structures for mild steel in acidic media indicated that they have good inhibition efficiency [15,16].

However, the length of the hydrocarbon chain attached to a corrosion inhibitor molecule can play a crucial role in modulating the hydrophobicity and film formation behavior of the corrosion inhibitors. This can have a direct effect on the adsorption mechanism and inhibition efficiency. The number of alkyl chains, the number of hydrocarbon units present in a chain, and the presence of π-bonds and heteroatoms attached directly to alkyl chains can have significance on wetting characteristics of a molecule and to the forte of adsorption [17,18].

One of the most important methods of determining the activity, interpretation and explanation mode of corrosion inhibitors are the DFT calculations and the molecular dynamics (MD) simulation [1]

In this work, three 8-(n-bromo-R-alkoxy)quinoline derivatives with long hydrocarbon chain were prepared and identified by proton and carbon NMR spectroscopy (^{1}H NMR and ^{13}C NMR) (Fig. 1). Thus, their influence on the MS corrosion in 1.0 M HCl medium was inspected by using electrochemical measurements. In addition, to determine the relationship between the anti-corrosion property from one side and the length hydrocarbon chain and electronic properties from another side of the synthesized compounds, DFT calculations and MD simulations were performed.

2. Experimental part

2.1. Synthesis and identification of organic compounds

The synthesis of this series of compounds was carried out by condensing 8-hydroxyquinoline (8-HQ) with an equivalent of compounds bearing nucleofuge groups in the presence of triethylamine (Et_3N) in tetrahydrofuran (THF) at 323±2 K for 5 h (Scheme 1).

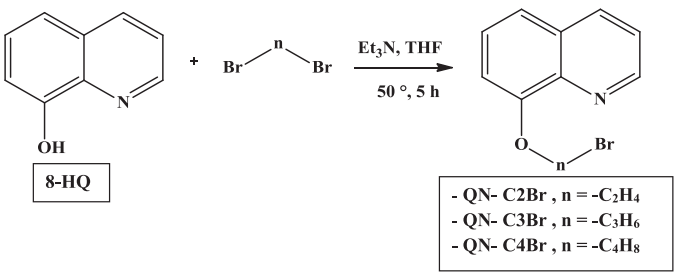

Scheme 1. Synthesis reaction of substituted 8-(n-bromo-R-alkoxy)quinoline compounds.

So, for a general operation mode, in a 50 mL flask containing 20 mL of tetrahydrofuran (THF), 1 mole of 8-hydroxyquinoline (8-HQ) and 2 moles of the compounds bearing a nucleofuge group are added in the presence of one mole of triethylamine (Et_3N). The reaction mixture is heated to 232±2 K, with magnetic stirring. The reaction is followed by TLC, using a mixture of hexane/dichloromethane (4: 6, v/v) as eluent. When, the latter indicates the complete consumption of the starting products after 8 hours of reaction. The reaction mixture is hydrolyzed with 20 mL of water (H_2O) and extracted with ethyl acetate (3×20 mL). The organic phases are combined, neutralized with an amount of $NaHCO_3$ to adjust the pH, then concentrated in a rotary evaporator under a water pump vacuum and cooled to 298±2 K, and then 15 mL of ether was added to crystallize the expected product in the form of needles. In addition, this equation and the description of these devices have been described in another publication [19]. The characterization of the obtained compounds with ^{1}H and ^{13}C NMR are indicated in Table 1. In addition, for this series of reactions, we present by way of example the ^{1}H and ^{13}C NMR spectra of compound QN-C2Br (Fig. 2).

2.2. Metal and preparation of solution

The material tested in this work is MS, where its chemical composition as follows (wt. %) : 0.11 % of C, 0.24 % of Si, 0.47 % of Mn, 0.12 % of Cr, 0.02 % of Mo, 0.1 % of Ni, 0.03 % of Al, 0.14 % of Cu, 0.06 % of W, < 0.0012 % of Co, < 0.003 % of V and 98.70 % of Fe [12]. The corrosive medium 1.0 M HCl was prepared via dilution of analytical grade HCl (Sigma Aldrich, 37 %) in distilled water. Four different concentrations (from 10^{-6} M to 10^{-3} M) of 8-(n-bromo-R-alkoxy)quinoline derivatives are prepared in a 1.0 M HCl.

2.3. Electrochemical study

Before each electrochemical experiment, the MS as working electrode with an exposed area of 1 cm^2, was polished with emery paper (up to 1200 grit), washed with acetone, then with distilled water, and finally dried in hot air as indicated in our previous works [20,21]. The electrochemical measurements were piloted in a glass cell equipped with three electrodes: MS, saturated calomel (SCE) and platinum as working, reference, and counter electrodes, respectively. The MS electrode immersed in a corrosive solution without and with each concentration of inhibitor at 298±2 K, for one hour until a steady-state open circuit potential (E_{OCP}) was reached using Galvanostat/Potentiostat PGZ 100 linked to computer-controlled, where the fitting was made with the Volta Master 4 software. In addition, the polarization curves were registered out at a constant scan rate of 0.5 mV/s, by polarization from – 900 mV/SCE to – 100 mV/SCE.

The corrosion kinetic parameters extracted by using the Tafel extrapolation method of the linear part of the cathodic and anodic

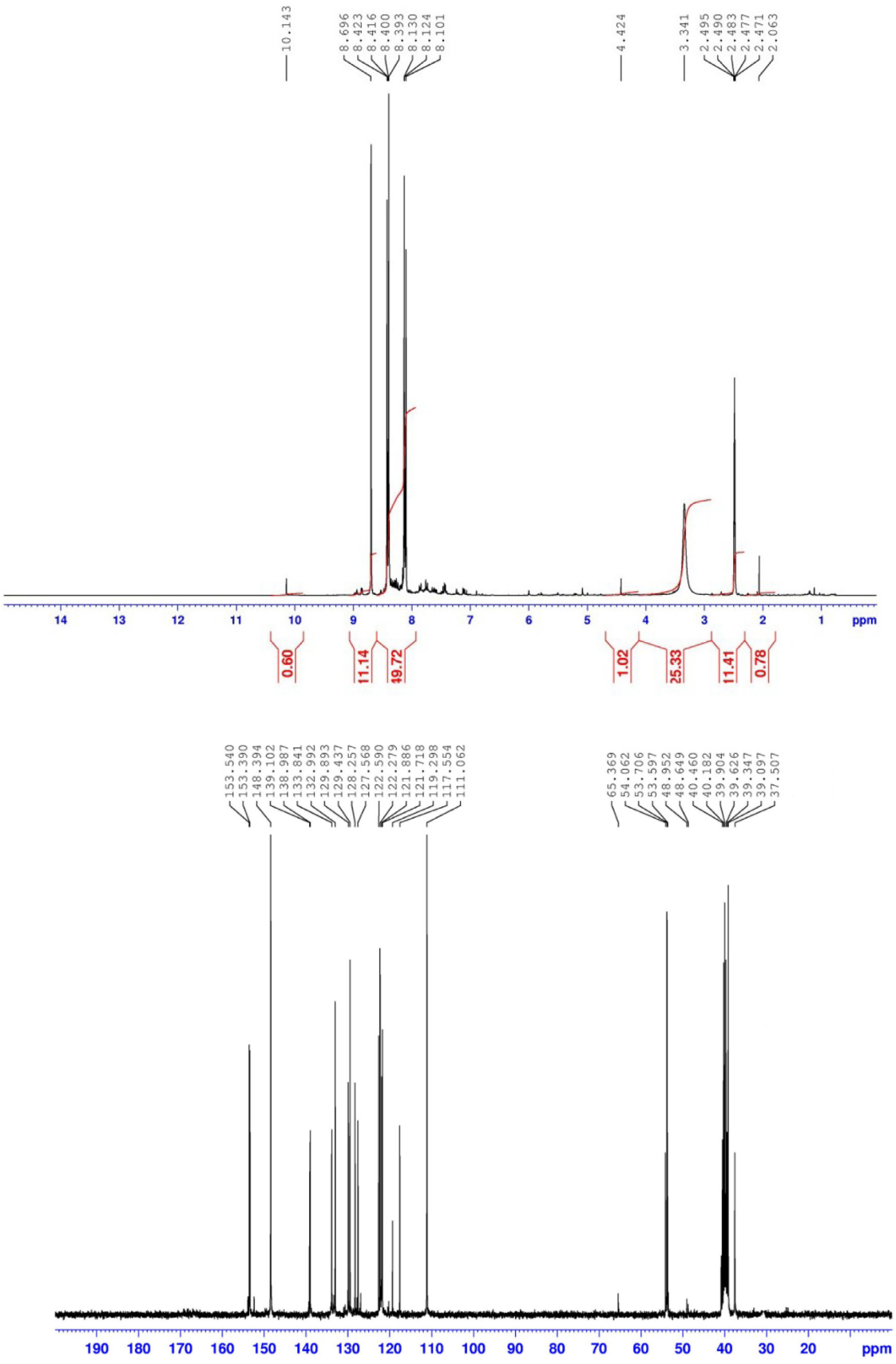

Fig. 2. 1H and 13C NMR spectra of 8-(2-bromoethoxy)quinoline (QN-C2Br).

Table 1
Name, abbreviation, and ^{1}H and ^{13}C NMR spectral data of the tested 8-(n-bromo-R-alkoxy)quinoline derivatives compounds.

Names	Abbreviations	RMN $^{1}H(\delta_{ppm})$, (DMSO-d_6)	RMN ^{13}C (δ_{ppm}), (DMSO-d_6)
8-(2-bromoethoxy) quinoline	QN-C2Br	4.42 (s, 2 H, CH_2) 2.06 (s, 1 H, CH-epoxy) 3.34 (s, 2 H, CH_2-O) 8.10-10.14 (m, 5 H, ArH-quinoline)	153.54 (C-OH) 65.36 (CH-epoxy) 54.06 (CH_2) 48.95 (CH_2-epoxy)
8-(3-bromopropoxy) quinoline	QN-C3Br	0.99 (s, 3 H, CH_3-Hydrocarbon chain) 1.15-1.29-1.30-1.33 (d, 30 H, CH_2- Hydrocarbon chain) 4.28 (s, 2 H, CH_2) 7.09-8.88 (m, 5 H, ArH-quinoline)	152.53 (C-OH) 15.03(CH_3-Hydrocarbon chain) 21.07-70.18(CH_2- Hydrocarbon chain) 78.19 (CH_2)
8-(4-bromobutoxy) quinoline	QN-C4Br	0.60 (s, 3 H, CH_3-Hydrocarbon chain)1,27-3.47 (d, 18 H, CH_2-Hydrocarbon chain) 5.21 (s, 2 H, CH_2) 7.00-8.91 (m, 5 H, ArH-quinoline).	155.49 (C-OH) 13.18 (CH_3- Hydrocarbon chain) 22.19-78.01(CH_2- Hydrocarbon chain) 78.50 (CH_2)

branches. The anti-corrosion efficiency calculated from the corrosion currents density values as follows:

$$\eta_{PP} = \frac{i^0_{corr} - i_{corr}}{i^0_{corr}} \times 100 \quad (1)$$

where i°_{corr} and i_{corr} are the corrosion current density values without and with each 8-hydroxyquinoline derivatives, respectively.

In addition, the EIS measurements were conducted using a transfer function analyzer, with a small amplitude a.c. signal (10 mV rms), over a frequency domain [100 mHz, 100 kHz] with 5 pts/decade. The EIS diagrams were analyzed and extrapolated by equivalent electrical circuits using Z-View software. Thus, the anti-corrosion efficiency, η_{EIS}, is calculated as follows:

$$\eta_{EIS} = \frac{R_{ct} - R^0_{ct}}{R_{ct}} \times 100 \quad (2)$$

where R°_{ct} and R_{ct} are the charge transfer resistance values without and with each 8-(n-bromo-R-alkoxy)quinoline derivatives, respectively.

2.4. UV-visible spectrophotometer

In order to characterize the free solution and inhibited after six hours of immersion at 298±2 K, the spectro-photometric method was carried out in 10^{-3} M of each inhibitor with 1.0 M HCl solution without and with MS sample by using a Beckman DU640 UV/Vis spectrophotometer.

2.5. Surface analysis

The morphology of the MS surface was obtained by the scanning electron microscopy (SEM) instrument (SEM, JOEL JSM-5500) at 25 keV with magnification (2000×) after six hours of immersion in 1.0 M HCl solution at 298 K without and with each inhibitor.

2.6. Computational Details

Conceptual Density Functional Theory [22] developed especially Parr provides great facilities to theoretical and computational chemists in terms of the approximate calculation of quantum chemical descriptors such as hardness (η), chemical potential (μ), electronegativity (χ), and softness (σ). In the theory, the aforementioned descriptors are given as the derivatives with respect to the number of electrons (N) of total electronic energy (E) at a constant external potential. To associate with ground state ionization energy (I) and electron affinity (A) values of chemical compounds the parameters, finite differences approach has been considered and last of all, the following equations are obtained [23].

$$\mu = -\chi = \left[\frac{\partial E}{\partial N}\right]_{v(r)} = -\left(\frac{I+A}{2}\right) \quad (3)$$

$$\eta = \frac{1}{2}\left[\frac{\partial^2 E}{\partial N^2}\right]_{v(r)} = \frac{I-A}{2} \quad (4)$$

$$\sigma = 1/\eta \quad (5)$$

To describe the electrophilic powers of atoms, ions and molecules, Parr, Szentpaly and Liu [24] proposed the electrophilicity index (ω) based on absolute hardness and the absolute electronegativity of chemical species. Then, Chattaraj [25] defined the nucleophilicity (ε) as the multiplicative inverse of the electrophilicity index.

$$\omega = \chi^2/2\eta = \mu^2/2\eta \quad (6)$$

$$\varepsilon = 1/\omega \quad (7)$$

Two new parameters called as the electron accepting power (ω^+) and electron donating (ω^-) power were imparted to science by Gazquez and coworkers [26]. These parameters depending on the ground state ionization energy and electron affinity values of chemical compounds are given as:

$$\omega^+ = (I+3A)^2/(16(I-A)) \quad (8)$$

$$\omega^- = (3I+A)^2/(16(I-A)) \quad (9)$$

Within the framework of Koopmans Theorem [27], ionization energies and electron affinities can be predicted with the consideration of the frontier orbital energies. The theory states that ionization energy is approximately negative value of HOMO orbital energy while electron affinity is approximately the negative value of LUMO orbital energy.

$$I = -E_{HOMO} \quad (10)$$

$$A = -E_{LUMO} \quad (11)$$

The polarizability (α) reported as one of the beneficial reactivity descriptors is calculated depending on diagonal components of the polarizability tensor.

$$\langle\alpha\rangle = 1/3[\alpha_{xx} + \alpha_{yy} + \alpha_{zz}] \quad (12)$$

The fraction of electrons transferred (ΔN) from the inhibitor molecule to the metallic surface and metal-inhibitor interaction energy ($\Delta\psi$) are important parameters in terms of the analysis of the anti-corrosion performances of molecules. These quantities are mathematically defined using the following formulae [28]:

$$\Delta N = \frac{\phi_{Fe} - \chi_{inh}}{2(\eta_{Fe} + \eta_{inh})} \quad (13)$$

$$\Delta\psi = -\frac{(\phi_{Fe} - \chi_{inh})^2}{4(\eta_{Fe} + \eta_{inh})} \quad (14)$$

In the given equations, Φ_{Fe} and η_{Fe} represent the work function and the absolute hardness of the metal and they are taken as 4.82 eV mol^{-1} and 0.0 eV mol^{-1}, respectively. The χ_{inh} and η_{inh} stand for the electronegativity and the hardness value of the 8-(n-bromo-R-alkoxy)quinoline derivative molecule, respectively.

Recently, some authors started to use the back-donation energy in corrosion inhibition studies. This parameters regarding to the hardness value of inhibitor molecule is given as:

$$\Delta E_{back-donation} = -\frac{\eta}{4} \quad (15)$$

Local reactivities of studied inhibitor molecules are analyzed using Fukui functions. Fukui function provides useful information in the determining of reactive sites of molecules. Atom condensed Fukui functions can be calculated with the help of the following equations. In the given equations, q_k is the charge on atom k [29].

$$f_k^{+} = q_k(N+1) - q_k(N) \text{(fornucleophilicattack)} \quad (16)$$

$$f_k^{-} = q_k(N) - q_k(N-1) \text{(forelectrophilicattack)} \quad (17)$$

$$f_k^{0} = \frac{q_k(N+1) - q_k(N-1)}{2} \text{(forradikalattack)} \quad (18)$$

2.7. Molecular dynamics studies

These studies provide important information about the nature of the interactions between inhibitor molecules and metal surfaces. In this paper, Molecular Dynamics Simulation studies were achieved with the help of Forcite Tools in Material Studio V.6 software. For the calculations made, Fe (110) surface due to its stabilized structure. For the calculations made using Andersen Thermostat providing an NTV set, the total simulation time and time step are 200 ps and 1 fs, respectively. The simulations were performed using COMPASS force field. The temperature for calculations was selected as 298 K. It is important to note that the designed supercells include Cl^- ions, H_3O^+ ions, H_2O molecules and 1 inhibitor molecule. In the calculation of adsorption energies (E_{ads}), the following equation was considered.

$$E_{ads} = E_{total} - (E_{solution+metal} + E_{inhibitor}) \quad (19)$$

wherein, E_{total} represents the total energy of the system. $E_{solution+metal}$ stands for the total energy of the system without any inhibitor molecule. $E_{inhibitor}$ is the energy of the inhibitor molecule.

Forcite Tools in Material Studio V.6 was used the estimation of mean square displacement (MSD). Calculations were performed with 30 inhibitors, 3 Cl^- and 3 H_3O^+ ions considering COMPASS force field. Van der Waals interactions were determined in the light of atom-based summation method. Ewald summation method was taken into consideration for the electrostatic inter-action calculation. For the calculation of MSD and diffusion coefficients (D), the following formulae are used [30].

$$MSD(t) = \left[\frac{1}{N}\sum_{i=1}^{N}|R_i(t) - R_i(0)|^2\right] \quad (20)$$

$$D = \frac{1}{6}\lim_{t\to\infty}\frac{dMSD(t)}{dt} \quad (21)$$

Here, $R_i(t)$ and $R_i(0)$ stand for the position vector of corrosive particle at time t and the position vector of corrosive particle at time 0, respectively. N is the total number of target molecules studied.

3. Results and discussion

3.1. Tafel polarization results

The I-E curves for MS in 1.0 M HCl solution at 298±2 K without and with the presence of QN-C4Br, QN-C3Br or QN-C2Br at various concentrations are presented in Fig. 3. Their extracted electrochemical parameters are illustrated in Table 2.

According to the figures and table, it is remarked that the E_{corr} of the MS is moved slightly towards the positive direction with QN-C2Br, QN-C3Br or QN-C4Br compound addition. In addition, the i_{corr} values decrease as the concentrations of the inhibitors increase. This observation clearly shows that QN-C2Br, QN-C3Br, and QN-C4Br are classified as anodic-type corrosion inhibitors. It is also

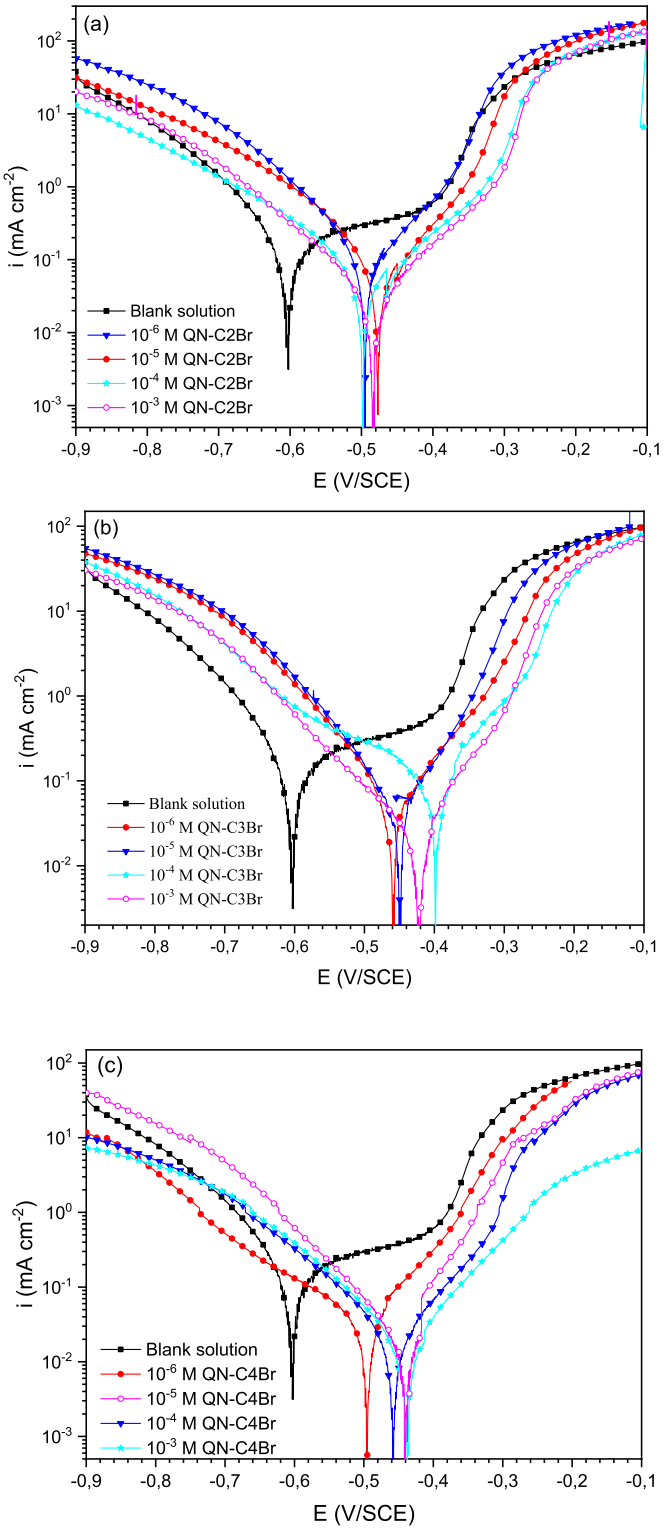

Fig. 3. I-E curves of MS in 1.0 M HCl without and with (a) QN-C2Br, (b) QN-C3Br and (c) QN-C4Br addition at different concentrations (T= 298±2 K).

seen that the η_{pp} values rise with the increase of QN-C2Br, QN-C3Br or QN-C4Br concentrations to reach the maximum value of 98.4 %, 98.7 % and 98.9 %, respectively. This excellent efficiency was explained by the presence of high electron densities on the derivative molecules due to the existence of the non-binding doublets of the heteroatoms -N, -O, and the electrons (π) of the aromas, which favors their adsorption process on the metal surface [31]. Moreover, it can be observed that the presence of the inhibitors causes

Table 2
Electrochemical parameters and inhibition efficiency values for MS in 1.0 M HCl without and with 8-(n-bromo-R-alkoxy)quinoline at defferent concentrations (T = 298±2 K).

Conc. (M)	-E_{corr} (mV_{SCE})		i_{corr} (μA cm^{-2}) -β_c (mV dec^{-1})	Tafel slopes β_a (mV dec^{-1})	η_{PP} (%)	θ
Blank solution						
0	545.00±2.13	949.0±5.22	101.00±5.25	74.9±4.22	-	-
QN-C2Br						
10^{-6}	476.9±2.17	107.51±4.33	113.1±4.13	60.9±2.15	88.7	0.8867
10^{-5}	495.0±3.22	97.26±5.21	82.2±3.28	53.2±2.86	89.8	0.8975
10^{-4}	483.13±4.75	17.97±2.13	78.9±3.24	53.8±1.88	98.1	0.9810
10^{-3}	497.64±5.13	15.54±2.25	45.72±2.27	60.0±2.04	98.4	0.9838
QN-C3Br						
10^{-6}	458.13±3.45	76.22±4.69	112.13±5.85	60.1±2.25	91.9	0.9197
10^{-5}	450.00±4.85	68.41±4.12	108.13±4.22	55.1±2.66	92.8	0.9279
10^{-4}	398.14±3.22	27.27±3.13	43.19±2.27	55.0±2.84	97.1	0.9713
10^{-3}	422.14±2.88	12.24±1.98	100.61±4.63	52.7±3.05	98.7	0.9871
QN-C4Br						
10^{-6}	495.80±3.78	120.69±5.11	294.7±5.68	35.80±2.44	87.3	0.8728
10^{-5}	457.9±4.13	30.43±2.58	134.8±4.77	41.56±2.53	96.8	0.9679
10^{-4}	437.8±2.44	14.61±2.07	100.6±3.28	53.8±5.11	98.5	0.9846
10^{-3}	440.0±3.45	10.76±1.13	74.0±3.63	87.91±2.25	98.9	0.9887

Table 3
EIS parameters and anti-corrosion efficiencies values for MS in 1.0 M HCl solution without and with various concentrations of 8-(n-bromo-R-alkoxy)quinolone derivatives at 298±2 K.

C (M)	R_s (Ω cm^2)	R_{ct} (Ω cm^2)	C_{dl} (μF cm^{-2})	n_{dl}	10^6 Q ($\Omega^{-1}S^n$ cm^{-2})	τ_{dl} (ms)	η_{EIS} %	$\chi^2 \times 10^4$
	Blank solution							
00	2.08	32.41±0.78	128.1	0.78±0.01	315.10±0.75	4.15	-	2.3
	QN-C2Br							
10^{-6}	1.74	186.92±1.28	82.28	0.81±0.01	129.10±0.85	15.38	81.8	2.4
10^{-5}	1.98	284.66±2.71	65.21	0.84±0.01	137.24±1.75	18.56	88.1	3.5
10^{-4}	0.25	445.31±1.11	64.32	0.87±0.01	105.97±0.98	28.64	92.4	3.6
10^{-3}	2.15	705.21±3.13	43.47	0.89±0.01	87.18±1.25	30.66	95.2	2.5
	QN-C3Br							
10^{-6}	2.19	218.51±4.11	152.23	0.81±0.01	216.19±1.88	39.35	84.4	5.1
10^{-5}	2.33	318.82±3.33	129.19	0.83±0.01	182.14±1.24	41.19	89.3	4.8
10^{-4}	1.29	348.50±2.12	111.28	0.88±0.01	133.50±1.09	38.78	90.3	2.7
10^{-3}	1.46	783.21±2.25	85.97	0.88±0.01	220.12±2.06	67.33	95.7	3.8
	QN-C4Br							
10^{-6}	1.22	534.41±3.25	124.14	0.83±0.01	274.40±1.96	66.34	93.6	3.1
10^{-5}	9.28	981.40±4.69	60.39	0.85±0.01	66.28±1.48	95.26	93.5	2.9
10^{-4}	1.80	1001.12±4.16	39.64	0.89±0.01	81.21±0.58	39.68	96.6	3.2
10^{-3}	7.34	1389.12±5.37	36.40	0.91±0.01	91.41±1.28	50.56	97.5	2.8

Table 4
Inhibition efficiency values for different organic compounds according to the literature.

Compounds	System	Conc. M	η %	References
5-(azidomethyl)-7- (morpholinomethyl)quinolin-8-ol	1 M HCl/mild steel	10^{-3}	90	[1]
(N-(1-methyl-2,4-dioxo-1,2,3,4- Tetrahydroquinazoline -3-carbonothioyl)propionamide	1 M HCl/mild steel	10^{-3}	88	[42]
2-(2,4-dichlorophenyl)-1,2,3,4- tetrahydroquinoxaline	1 M HCl/mild steel	10^{-3}	91	[43]
	QN-C2Br, n = -C_2H_5			
QN-C3Br, n = -C_3H_7				
QN-C4Br, n = -C_4H_9	1.0 M HCl/mild steel	10^{-3}	95.2 95.7 97.5	This work

Table 5
Values of electrochemical and activation parameters the MS dissolution in 1.0 M HCl without and with 10^{-3} M of each 8-(n-bromo-R-alkoxy)quinoline.

T (K)	E_{corr} mV_{SCE}	i_{corr} μA/cm^2	η_{PDP} %	E_a kJ mol^{-1}	ΔH_a kJ mol^{-1}	ΔS_a J mol^{-1} K^{-1}	R^2	ΔG°_{ads} kJ mol^{-1}
Blank solution								
298±2	545	949	–	33.08	30.42	-85.70	–	–
308±2	487	1400	–					
318±2	490	2550	–					
328±2	478	3000	–					
QN-C2Br								
298±2	497.64	15.54	98.36	111.40	108.42	124.95	0.9999	-47.58
308±2	486.37	174.12	86.25					
318±2	505.74	269.74	84.59					
328±2	510.9	1275.4	51.32					
QN-C3Br								
298±2	422.14	12.24	94.2	107.05	104.45	127.89	0.9998	-47.78
308±2	438.96	80.41	90.69					
318±2	444.15	201.23	82.52					
328±2	437.31	720.31	82.04					
QN-C4Br								
298±2	440.0	10.76	98.87	87.23	84.63	56.95	0.9998	-47.42
308±2	434.78	21.53	98.30					
318±2	445.44	58.51	96.66					
328±2	553.96	281.92	89.34					

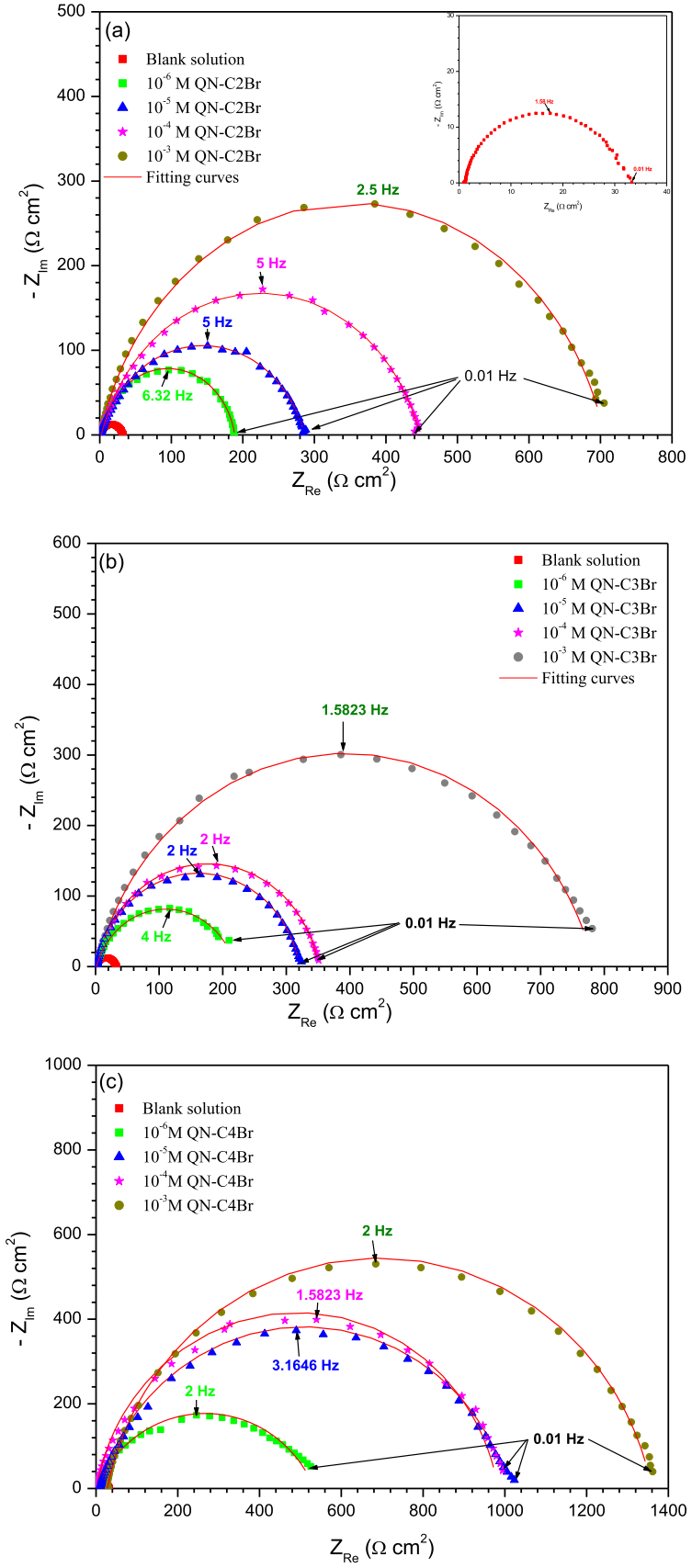

Fig. 4. Nyquist impedance diagrams for MS in 1.0 M HCl after one hour of immersion at the open circuit potential in the absence and presence of (a) QN-C2Br, (b) QN-C2Br and (c) QN-C2Br at different concentrations (T= 298±2 K).

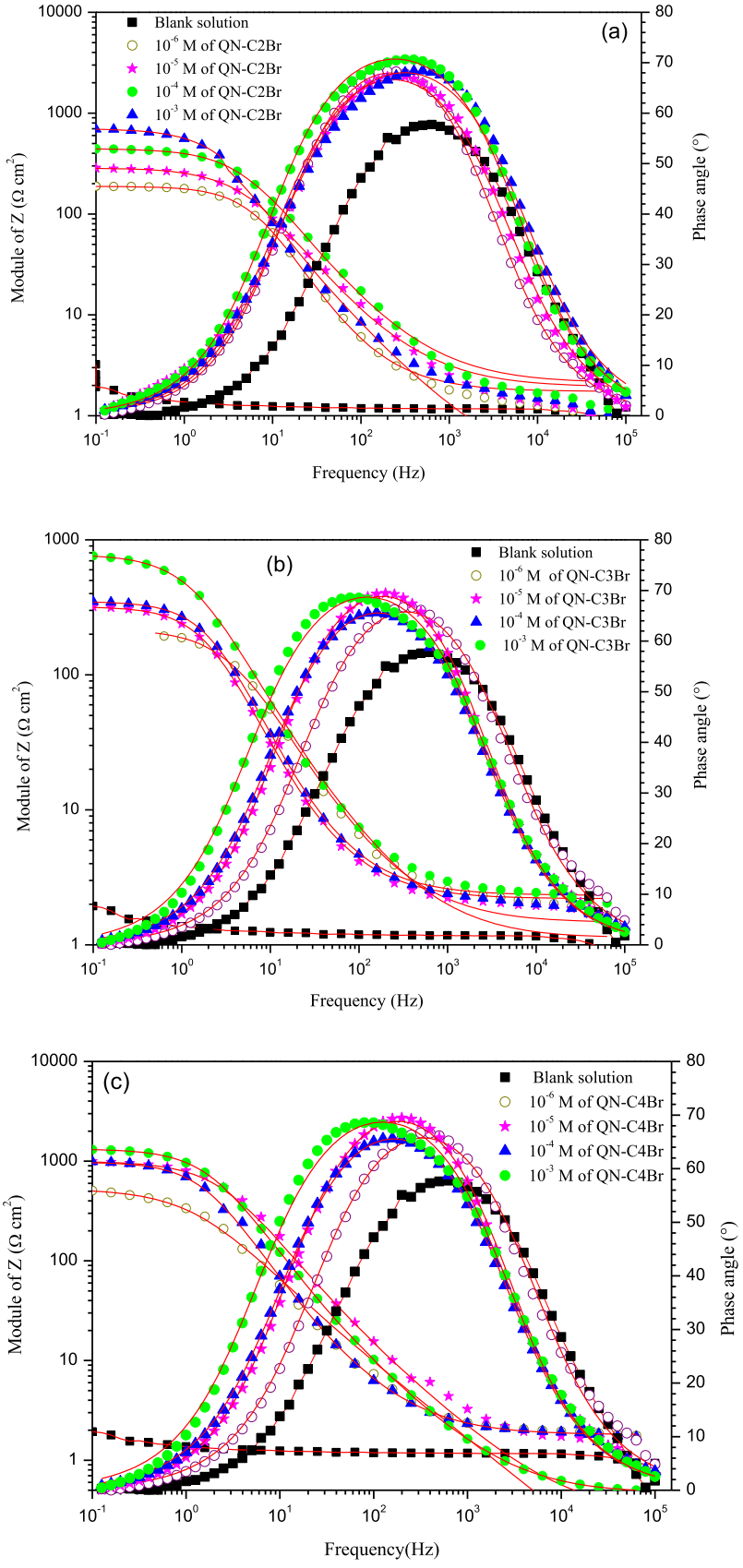

Fig. 5. Bode-phase presentation for MS in 1.0 M HCl after one hour of immersion at the open circuit potential in the absence and presence of (a) QN-C2Br, (b) QN-C2Br and (c) QN-C2Br at different concentrations (T= 298±2 K).

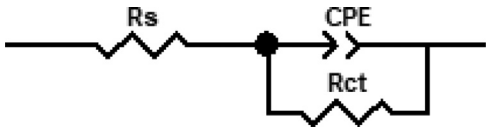

Fig. 6. The proposed circuit for the studied MS/ acidic medium/inhibitor system.

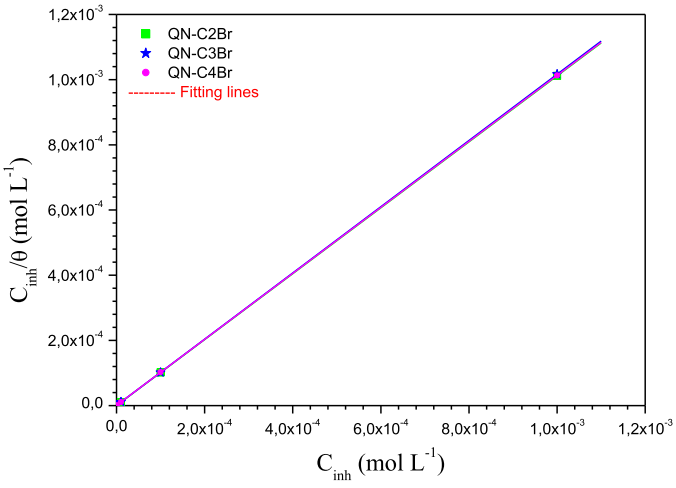

Fig. 7. Langmuir adsorption isotherm plots for MS in 1.0 M HCl with the presence of QN-C2Br, QN-C3Br or QN-C4Br at 298±2 K.

a slight decrease in the cathodic Tafel slope values (β_c), compared to that obtained for free solution, indicating a slight change in the hydrogen reduction mechanism [31]. On the other hand, the anodic Tafel slope values (β_a) stay almost unchanged with QN-C2Br, QN-C3Br or QN-C4Br addition, indicating no change in the MS dissolution [32]. This result indicates that these 8-(n-bromo-R-alkoxy)quinoline derivatives act by simply blocking the active sites of the available surface area. On the other hand, the inhibitor reduces the surface area of the metallic surface against corrosion without changing the mechanism, by causing only the inactivation of part of the surface [33].

However, it is obtained, such as mentioned above that the anti-corrosion efficiency follows the trend: QN-C4Br > QN-C3Br > QN-C2Br. In fact, the length of the hydrocarbon chain of the inhibitor molecule can product an essential role in the hydrophobicity modulating and its film formation behavior. So, the number of alkyl chains, the number of hydrocarbon units present in a chain, and the presence of π-bonds and heteroatoms devoted directly to alkyl chains can have meaning on wetting characteristics of a molecule and to the great adsorption [34].

3.2. EIS study

Many studies have shown that EIS are susceptible to disclose the elementary stages involved in the overall corrosion and/or anti-corrosion processes [33]. This method can be explained the chemical or electrochemical processes, developing through the films formed. Thus, Nyquist diagrams of MS immersed in 1.0 M HCl electrolyte without and with the addition of different concentrations of compounds QN-C2Br, QN-C3Br or QN-C4Br are shown in Fig. 4. It is observed that the obtained impedance diagrams were formed by one not perfect semi-circle, and this is attributed to the difference in frequency dispersion due to the heterogeneity of the electrochemical system, which is the result of the roughness, impurities, dislocations, inhibitor adsorption, and/or the formation of porous layers [35]. In the Bode phase plots, just one peak is viewed, indicating one time constant (Fig. 5). The peak height increases with the QN-C2Br, QN-C3Br or QN-C4Br concentrations, revealing the powerful adsorption of these compounds on MS surface. Besides,

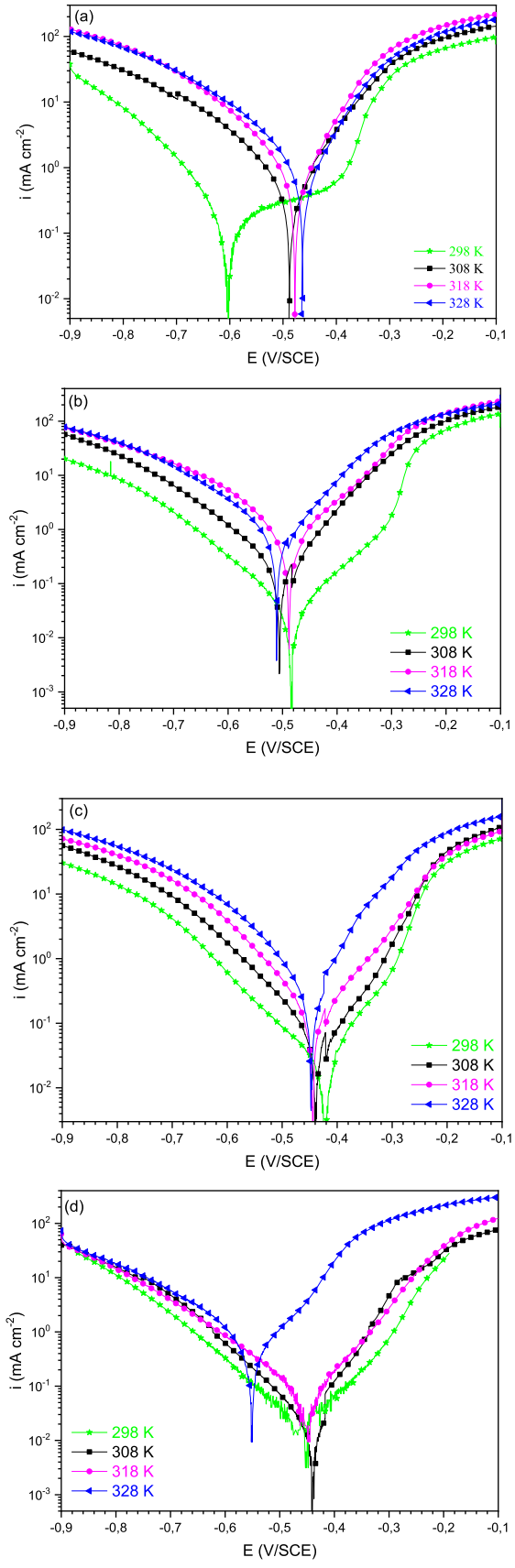

Fig. 8. Stationary polarization curves of MS 1.0 M HCl at different temperature (a) without and with 10−3 M of (b) QN-C2Br, (c) QN-C3Br and (d) QN-C4Br.

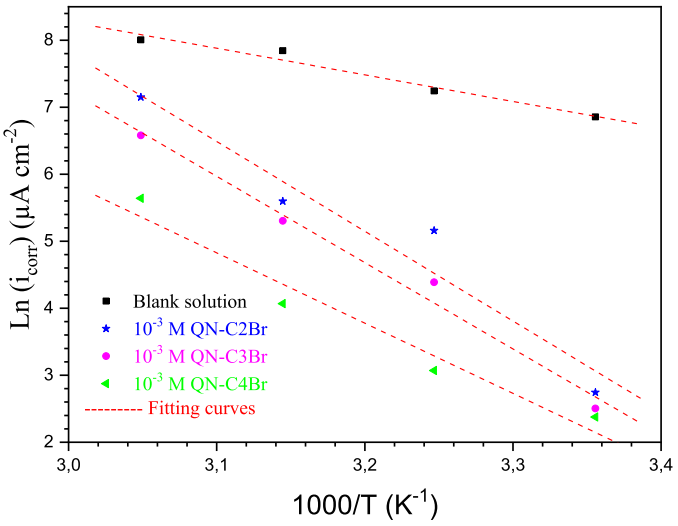

Fig. 9. Arrhenius curves for MS in 1.0 M HCl without and with 10−3 M of 8-(n-bromo-R-alkoxy)quinoline derivatives.

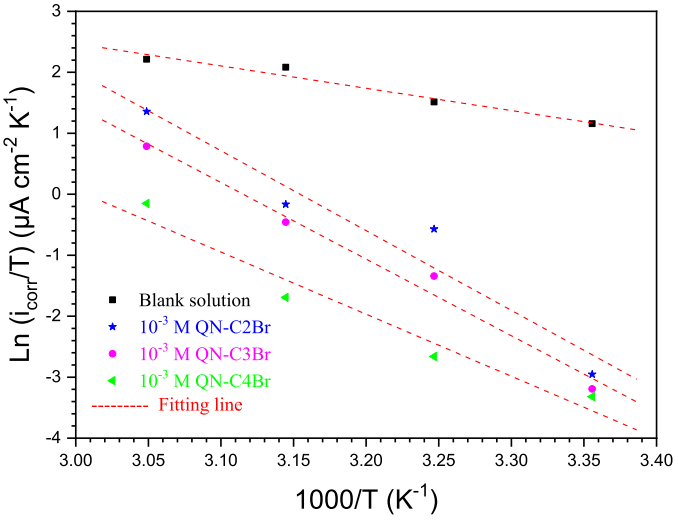

Fig. 10. Transition-state curves for MS in 1.0 M HCl without and with 10−3 M of each 8-(n-bromo-R-alkoxy)quinoline.

the values of log |Z| increase pointedly at low frequencies with increasing of testing products dose, and that the form of the plots stays unchanged in the presence of all synthesized compounds.

However, the proposed electrical equivalent circuit which endorsed us to make a good explanation of the obtained impedance spectrum is presented in Fig. 6. This circuit shows a constant phase element in parallel with a charge transfer resistance (R_{ct}), where the whole is in series with another solution resistance (R_s). Besides, the chi-squared was employed to determine the precision of the simulated data, the small chi-squared values ($\approx 10^{-4}$) (Table 3) found for all the results indicate that the simulated are well correlated with the experimental data.

According to Table 3, it can make the following remarks: the transfer resistance (R_{ct}) values increase with increasing of 8-(n-bromo-R-alkoxy)quinoline derivatives concentration. This increase indicated that the barrier layer formed of the protected sample seems to be more resistant [36]. In addition, it is seen that the double layer capacities (C_{dl}) decrease with the increase of inhibitor concentrations. This decrease was associated with the organic molecule adsorption on the MS surface [37], which has the effect of the reduction the dielectric constant (ε) of the medium and/or the increase of the double layer thickness (d), which is represented in Helmotz's model [37]:

$$C_{dl} = \frac{\varepsilon \times \varepsilon_0}{d} \times S \tag{22}$$

Conversely, the constant of the relaxation time (τd) of the charge transfer process was determined like as [38]:

$$\tau_d = C_{dl} R_{ct} \tag{23}$$

So, it is noted that this constant (τ_d) value for the blank solution (4.15) increases with the 8-(n-bromo-R-alkoxy)quinoline derivatives concentration (15.38– 67.33), signifying that the adsorption process rate of inhibitor molecules at the MS surface, is slow [39]. Additionally, it can be observed that the n_{dl} value of the blank electrolyte (0.78) rises with the presence of inhibitors (0.81 – 0.91), suggesting the reduction of surface inhomogeneities due to the inhibitors molecule adsorption on the MS surface [40,41].

On the other hand, it can be noted that the anti-corrosion efficiency at 10^{-3} M of each 8-hydroxyquinoline derivative follows the tendency: QN-C4Br (97.5 %) > QN-C3Br (95.7 %) > QN-C2Br (95.2 %). This classification confirms this obtained by plotting the stationary polarization curves. However, Table 4 represents the inhibition efficiency values of the some selected similar organic compounds used for the protection of mild steel in 1.0 M HCl compared to our tested compounds. By comparing these data, it is seen that QN-C2Br, QN-C3Br and QN-C2Br are the best inhibitor used

Table 6
The estimated quantum chemical descriptors for the studied 8-(n-bromo-R-alkoxy)quinoline molecules.

	6-31G			6-31G(d)			6-31++G(d)		
	QN-C2Br	QN-C3Br	QN-C4Br	QN-C2Br	QN-C3Br	QN-C4Br	QN-C2Br	QN-C3Br	QN-C4Br
E_{HOMO} (eV)	-5.8023	-5.7517	-5.6940	-5.7150	-5.6671	-5.6113	-5.9991	-5.9547	-5.8989
E_{LUMO} (eV)	-1.5002	-1.4858	-1.4341	-1.3913	-1.3775	-1.3268	-1.7595	-1.7513	-1.7018
I	5.8023	5.7517	5.6940	5.7150	5.6671	5.6113	5.9991	5.9547	5.8989
A	1.5002	1.4858	1.4341	1.3913	1.3775	1.3268	1.7595	1.7513	1.7018
ΔE (eV)	4.3022	4.2660	4.2600	4.3237	4.2896	4.2845	4.2396	4.2034	4.1971
η (eV)	2.1511	2.1330	2.1300	2.1618	2.1448	2.1422	2.1198	2.1017	2.0986
σ (eV^{-1})	0.4649	0.4688	0.4695	0.4626	0.4662	0.4668	0.4717	0.4758	0.4765
χ (eV)	3.6513	3.6187	3.5640	3.5532	3.5223	3.4691	3.8793	3.8530	3.8004
μ (eV^{-1})	-3.6513	-3.6187	-3.5640	-3.5532	-3.5223	-3.4691	-3.8793	-3.8530	-3.8004
ω	3.0988	3.0697	2.9818	2.9200	2.8922	2.8089	3.5496	3.5319	3.4411
ε	0.3227	0.3258	0.3354	0.3425	0.3458	0.3560	0.2817	0.2831	0.2906
ω^+	1.5421	1.5270	1.4661	1.4136	1.3992	1.3421	1.8749	1.8680	1.8032
ω^-	5.1934	5.1458	5.0301	4.9667	4.9215	4.8111	5.7542	5.7210	5.6036
ΔN	0.2717	0.2816	0.2948	0.2930	0.3025	0.3153	0.2219	0.2300	0.2429
$\Delta\psi$	-0.159	-0.169	-0.185	-0.186	-0.196	-0.213	-0.104	-0.111	-0.124
$\Delta E_{b\text{-}d}$	-0.5378	-0.5332	-0.5326	-0.5404	-0.5362	-0.5356	-0.53	-0.5254	-0.5246
α	135.75	147.97	159.28	141.88	154.08	165.50	163.59	177.15	189.83

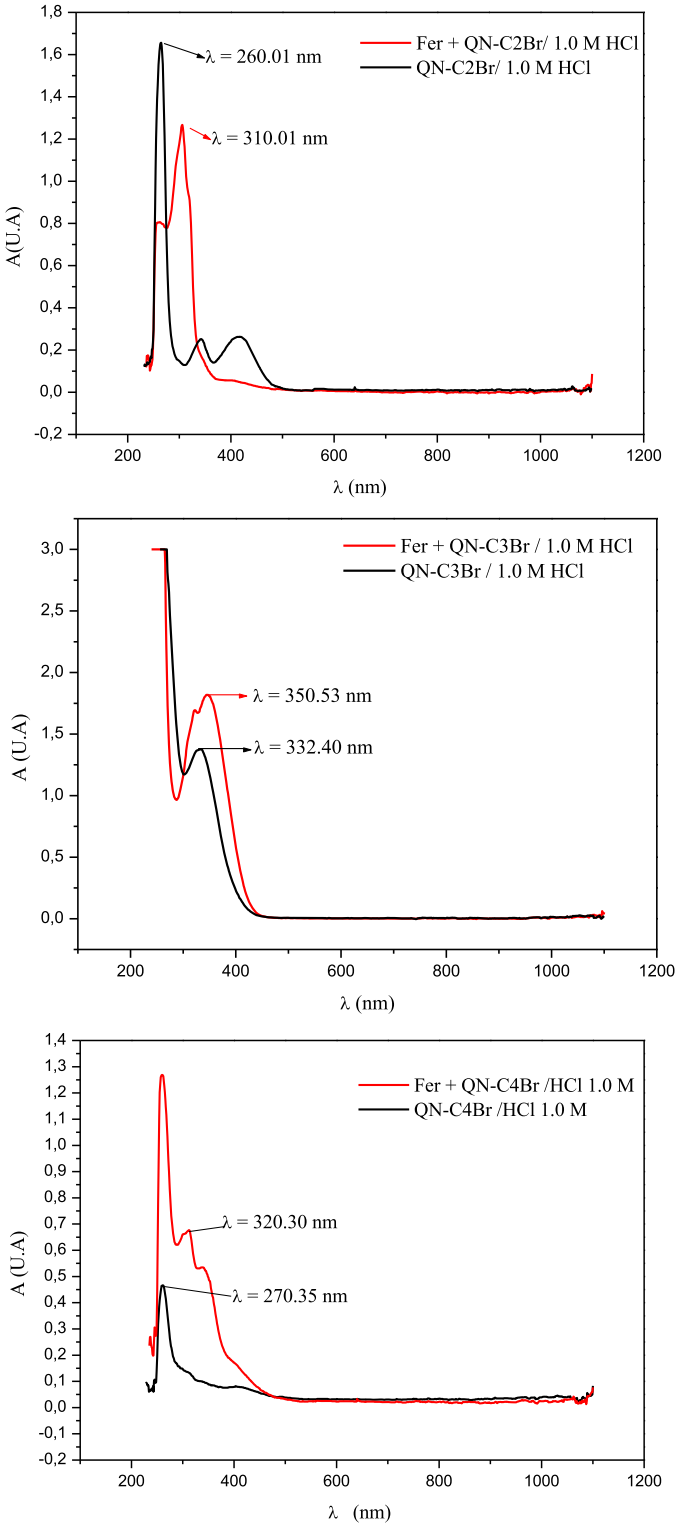

Fig. 11. UV-visible spectra of 1.0 M HCl solution containing 10−3 M of QN-C2Br, QN-C3Br or QN-C4Br before (black) and after (red) after 6 hours of MS immersion.

for mild steel in 1.0 M HCl. These performances can be obtained by the length hydrocarbon chain and by the presence of bromide atom.

3.3. Adsorption isotherm

To take more supplementary information for the interaction between inhibitor molecules and metal surface, numerous adsorption isotherms were tried, where the coverage surface (θ) was estimated as follows: $\theta = \eta_{PP}/100$ (Table 2). So, it is obtained that the plot of C_{inh}/θ versus C_{inh}, presented in Fig. 7, indicates a linear evolution (where R^2 near to 1 as indicated in Table 4), demonstrating that the adsorption of all 8-(n-bromo-R-alkoxy)quinoline molecules follows to the Langmuir isotherm, where is as follows:

$$\frac{C_{inh}}{\theta} = \frac{1}{K_{ads}} + C_{inh} \tag{24}$$

Where C_{inh} is the concentration of the used inhibitor (mol L^{-1}) and K_{ads} is the equilibrium constant for the adsorption and the desorption process, which is linked to the free energy of the adsorption (ΔG_{ads}) :

$$K_{ads} = \frac{1}{55.55} \exp\left(\frac{-\Delta G_{ads}}{RT}\right) \tag{25}$$

Where R is the constant of universal gas, 55.55 is the water concentration in solution (mol L^{-1}), and T is the absolute temperature (K).

Allowing to the above obtained result, it can be said that the molecules of the tested 8-(n-bromo-R-alkoxy)quinoline compounds hold and establish a monolayer at their optimum concentration without interaction between the holder species on the MS surface. It is found that that ΔG_{ads} values are about - 47.58 kJ mol^{-1}, - 47.78 kJ mol^{-1}, and - 47.42 kJ mol^{-1} for QN-C2Br, QN-C3Br, and QN-C4Br, respectively. So, these high negative values of ΔG_{ads} indicate the spontaneous and high adsorption capacity of 8-(n-bromo-R-alkoxy)quinoline derivative molecules on the MS surface and discloses the formed layer stability on the MS surface [21]. Rendering to the literature, the 8-(n-bromo-R-alkoxy)quinoline derivative molecules act via a chemisorption process on the MS surface. This is as a consequence of partition and/or change of electrons of π-electrons of the heterocyclic ring and/or free electrons of nitrogen and/or oxygen atoms of the 8-(n-bromo-R-alkoxy)quinoline derivative molecules to the unoccupied d-orbits of MS surface atoms to establish a co-ordinate bond [44,45].

3.4. Temperature solution effect and activation parameters

The effect of temperature solution is one of the most practical methods for investigation of MS corrosion, and the most exploitable technique for extracting of the activation parameters (E_a, ΔH_a and ΔS_a). Fig. 8 represents the stationary polarization curves obtained for MS in 1.0 M HCl solution without and with the optimum concentration of each compound of QN-C4Br, QN-C3Br and QN-C2Br; and their extracted and calculated parameters are illustrated in Table 5.

It is observed that the increase of temperature solution shifts the E_{corr} more negative direction in the presence of each inhibitor, while it moves to the positive direction in the case of blank solution; with the increase of i_{corr} for all cases. So, the increase in temperature causes the de-sorption of the studied 8-(n-bromo-R-alkoxy)quinoline molecules from the MS surface. In addition, from Table 5, it is detected that the η_{pp} values decrease slowly with temperature solution, but they remain high even at high temperature.

Though, the parameters of the activation process (Ea, ΔHa, and ΔSa) were calculated according to the literature [46]:

$$i_{corr} = A \exp\left(-\frac{E_a}{RT}\right) \tag{26}$$

$$i_{corr} = \frac{RT}{Nh} \exp\left(\frac{\Delta S_a}{R}\right) \exp\left(-\frac{\Delta H_a}{RT}\right) \tag{27}$$

Where A is the Arrhenius pre-exponential constant, R represents the universal gas constant, T is the absolute temperature, h is the Planck's constant, and N is the number of Avogadro.

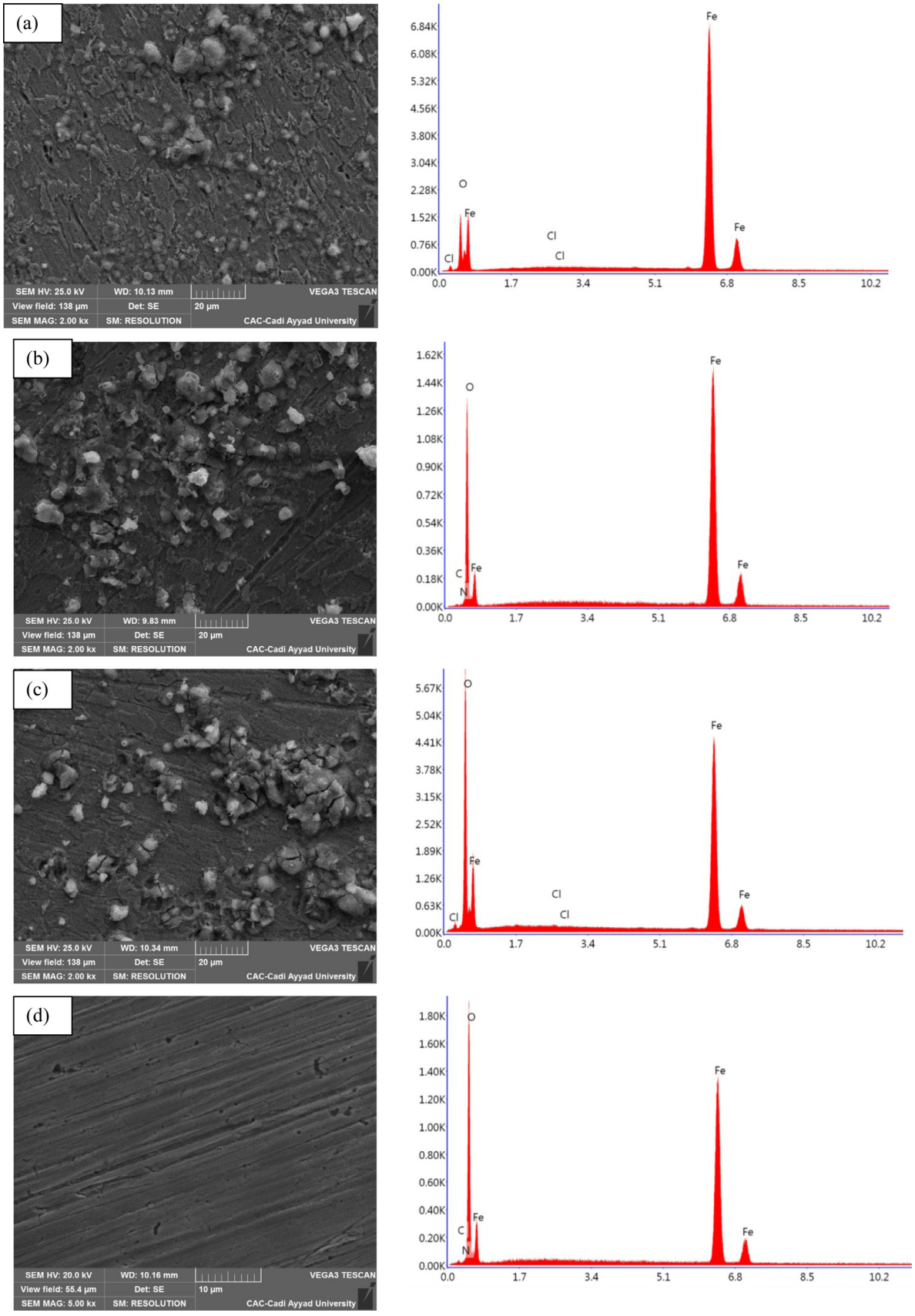

Fig. 12. Surface morphology and EDAX spectra of MS after 6 hours immersion in (a) blank solution of 1.0 M HCl and with 10−3 M of (b) QN-C2Br, (c) QN-C3Br and (d) QN-C4Br.

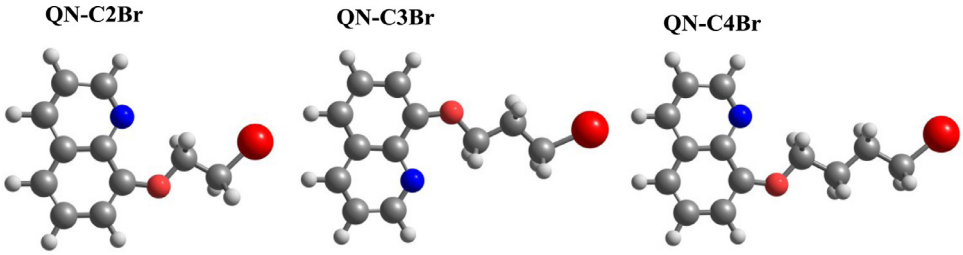

Fig. 13. Optimized structures of the studied 8-(n-bromo-R-alkoxy)quinoline molecules.

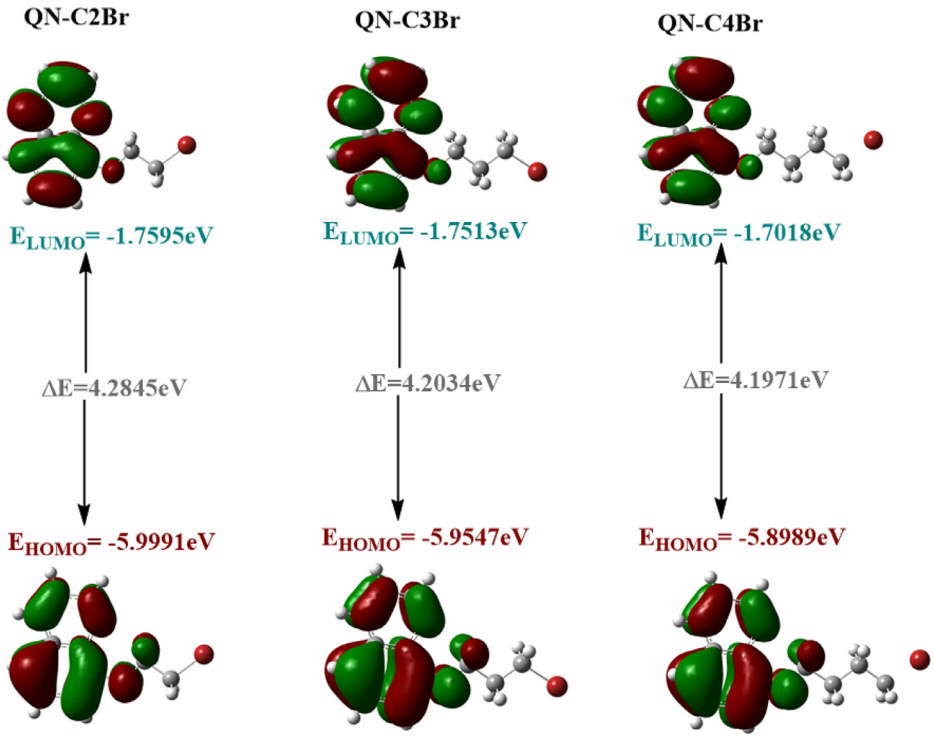

Fig. 14. Frontier molecular orbitals of the studied 8-(n-bromo-R-alkoxy)quinolone derivatives molecules.

Figs 9 and 10 represent the relationship between ln (i_{corr}) or ln (i_{corr}/T) and 1000/T for the MS in molar hydrochloric solution without and with the optimum concentration (10^{-3} M) of QN-C2Br, QN-C3Br or QN-C4Br. The obtained parameters of the activation process are presented in Table 5.

Table 5 showed that the values of Ea in the presence of 10−3 M of QN-C2Br (111.40 kJ mol−1), 10−3 M of QN-C3Br (107.05 kJ mol−1) and 10−3 M of QN-C4Br (84.63 kJ mol−1), are greater than that in their absence (33.08 kJ mol−1). This increase in Ea can be interpreted by physical adsorption of 8-(n-bromo-R-alkoxy)quinoline derivative molecules on the MS surface [47]. These communications are caused by the establishment of an energy barrier when the three 8-(n-bromo-R-alkoxy)quinoline are added to the corrosive electrolyte [48].

However, the obtained activation enthalpy values (ΔH_a) in the presence of three compounds are greater than this of the free solution, which indicates that the corrosion reaction of the process is spontaneous from the reagents to the compounds. Moreover, it is noted that all ΔH_a values are positives, demonstrating the endothermic nature of the corrosion process, and the MS dissolution became more difficult [35].

Additionally, the calculated ΔS_a values in the case of 10^{-3} M of QN-C2Br (124.95 J mol^{-1} K^{-1}), 10^{-3} M of QN-C3Br (127.89 J mol^{-1} K^{-1}) and 10^{-3} M of QN-C4Br (84.63 J mol^{-1} K^{-1}), are higher than that for the blank solution (-85.70 J mol^{-1} K^{-1}), indicating the rise of the solvent entropy. This may take place by the disinterest of great numbers of water molecules from the MS surface, and favorite the ordered of the larger inhibitors molecules adsorbed on the metal surface [49].

3.5. Solution analysis

The absorption of monochromatic light is a suitable method for identification of complex ions, the absorption of light is proportional to the concentration of the absorbing species. For routine analysis a simple conventional technique based on UV–vis absorption is the more sensitive direct spectrophotometric detection. Change in position of the absorption maximum and or change in the value of absorbance indicates the formation of a complex between two species in solution.

To better understand the binding mechanism between inhibitor molecules and iron ions in the acid solution, we use UV-visible spectroscopy. The electron absorption spectra of QN-C2Br, QN-C3Br and QN-C4Br solutions Fig. 11, before immersion of MS in 1.0 M HCl solution show visible absorption bands 260.01 nm, 332.40 nm and 270.35 nm for QN-C2Br, QN-C3Br and QN-C4Br, respectively. This band may be assigned to the $\pi-\pi^*$ transition, involving the whole electronic structure system of the substituted 8-(n-bromo-R-alkoxy)quinoline compound with a considerable charge transfer character [50].

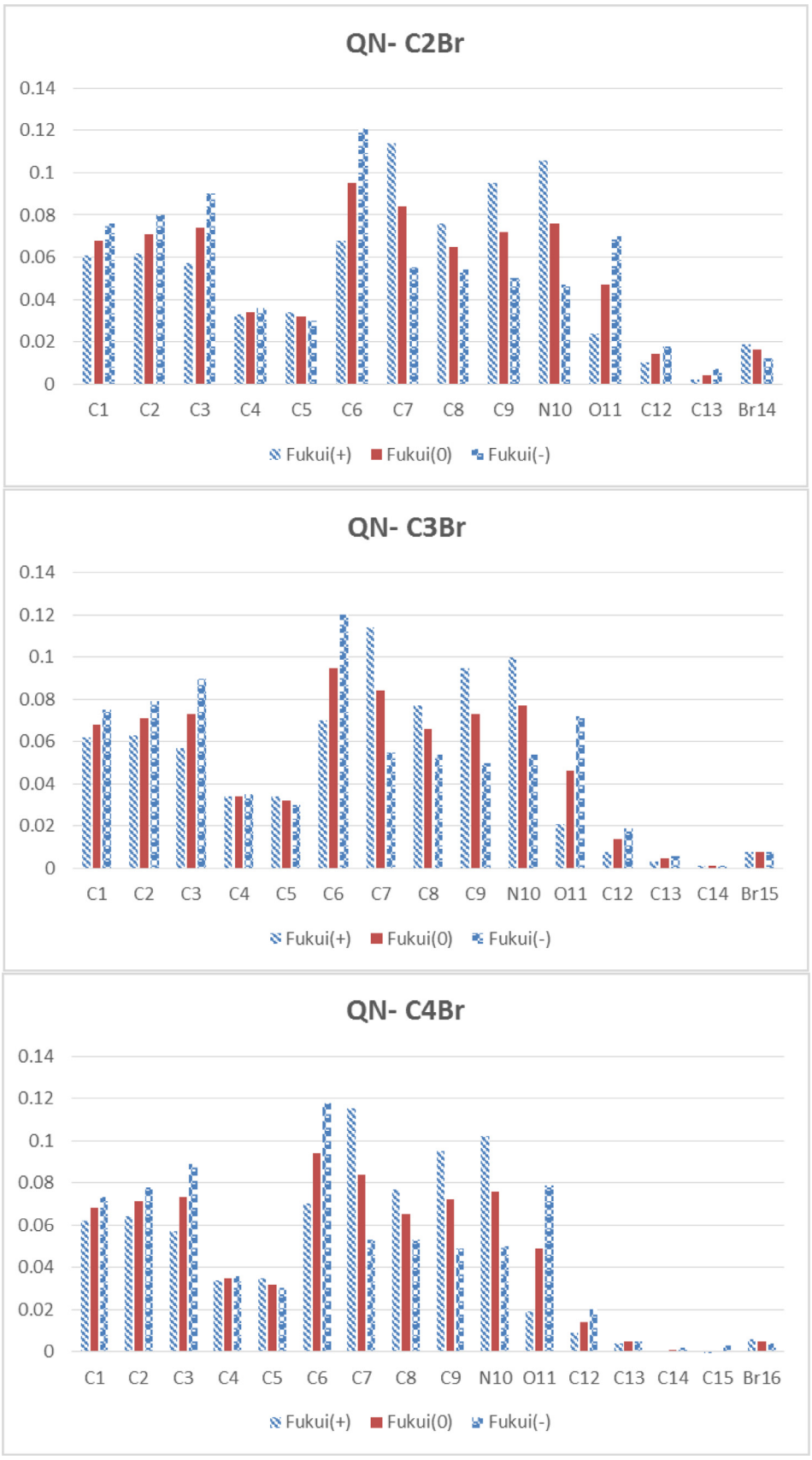

Fig. 15. Fukui indices of the studied 8-(n-bromo-R-alkoxy)quinolone inhibitors in aqueous phase using GGA/BLYP method with DNP 3.5 basis set.

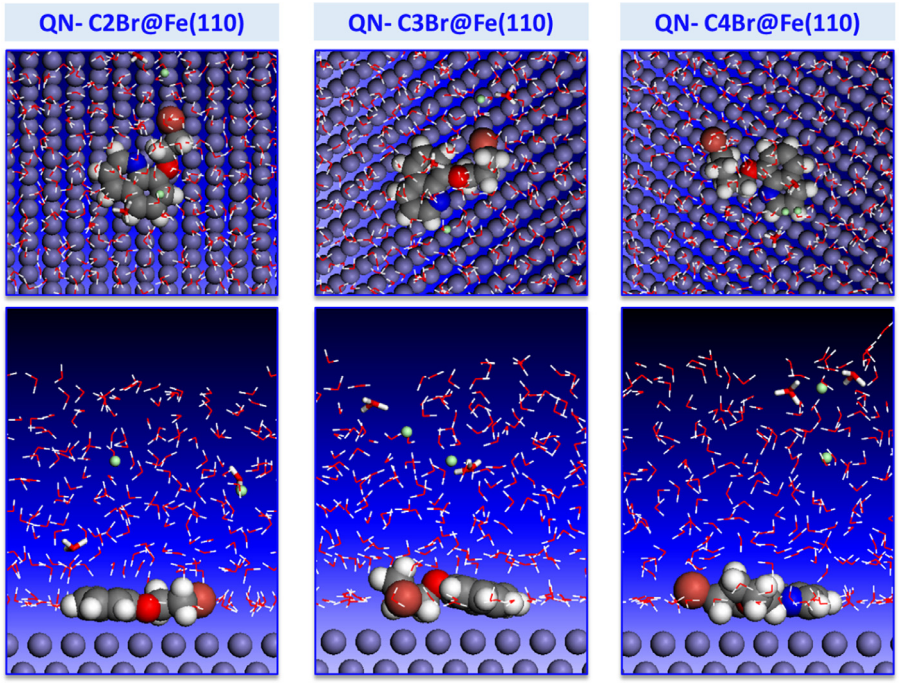

Fig. 16. Most stable adsorption configuration of the examined 8-(n-bromo-R-alkoxy)quinolone derivatives inhibitors on Fe (110) surface.

Table 7
E_{Total}, $E_{Solution+metal}$, $E_{Inhibitor}$ and E_{ads} of the studied inhibition systems (kcal mol^{-1}).

Inhibitors	E_{Total}	$E_{Solution+metal}$	$E_{Inhibitor}$	E_{ads}
QN-C2Br	-2177.739	-2157.418	107.719	-128.039
QN-C3Br	-2203.220	-2178.085	110.560	-135.695
QN-C4Br	-2135.334	-2100.792	109.280	-143.822

Table 8
Diffusion coefficient (D) of Cl^- and H_3O^+ ions through the inhibitors membrane.

Inhibitors	D (cm^2/s) Cl^-	H_3O^+
QN-C2Br	8.14158×10^{-6}	9.02778×10^{-6}
QN-C3Br	1.23783×10^{-6}	6.09493×10^{-6}
QN-C4Br	7.55535×10^{-8}	1.75772×10^{-6}

However, after 6 hours of immersion of specimen in aggressive solution Fig. 11, the absorption bands λ_{max} underwent a bathochromic shift from 260.01 nm, 332.40 nm and 270.35 nm at 310.01 nm and 350.51 nm at 320.30 nm, respectively for QN-C2Br, QN-C3Br and QN-C4Br. Our experimental findings are good evidence for the possibility of the formation of a complex among Fe^{2+} and inhibitors in 1.0 M HCl.

3.6. Surface analysis

The SEM micrographs of the MS surface in 1.0 M HCl medium after 6 hours of immersion time and at 298±2 K in the absence and presence of 10^{-3} M of QN-C2Br, QN-C3Br or QN-C4Br, were presented in Fig. 12a-d. The observation of the image of MS in the acidic solution without QN-C2Br, QN-C3Br or QN-C4Br, showed that the state surface was intensely damaged, due to quick corrosion degradation (Fig. 12a). On the other hand, in the presence of QN-C2Br, QN-C3Br or QN-C4Br at 10^{-3} M (Figs 12b, c and d), it is observed that the surface is covered with the presence of the traces in the form of a plate, indicating the presence of the organic products. This remark showed that the corrosion protection is due to the formation of a deposit by the formation of a film of the molecule inhibitors on MS surface. In addition, the elemental analyzes obtained by EDAX analysis, showed that the heteroatoms such as N, C and O present in the molecules QN-C2Br, QN-C3Br and QN-C4Br are in contact with the MS surface and could serve as adsorption sites.

3.7. Theoretical studies

Fig. 13 represents the optimized structures of QN-C2Br, QN-C3Br and QN-C4Br, which have obtained at B3LYP/ 6-31++G(d) calculation level.

It is imperative to note that quantum chemical parameters like frontier orbital energies, hardness, softness, electronegativity, chemical potential, electrophilicity, nucleophilicity, electrodonating power, electroaccepting power, polarizability, the fraction of electrons transferred from inhibitor molecule to metal surface, metal-inhibitor interaction energy, back-donation energy, and Fukui indices are usually considered in the extrapolation of anti-corrosion performances of organic and inorganic compounds. The calculated global reactivity properties of the studied molecules are given in Table 6 as detailed. Calculations were repeated at B3LYP/ 6-31G(d), B3LYP/ 6-31G, B3LYP/ 6-31++G(d) calculation levels for comparisons that will be made.

According to Molecular Orbital Theory, HOMO and LUMO orbital energies can be used for the prediction of electron donating and electron accepting abilities of molecules. It should be noted that HOMO orbital represents the electron donating ability and its high values belong to good corrosion inhibitor. In contrast, low LUMO orbital energy values show that the molecule doesn't want to give the electrons. It is apparent from the data presented for frontier orbital energies in the table given above, the anti-corrosion performances of the studied 8-(n-bromo-R-alkoxy)quinoline molecules obey the order: QN-C4Br > QN-C3Br > QN-C2Br. This order is very harmonious with the experimental obtained results.

It is well-known that quantum chemical descriptors like hardness, softness, polarizability and energy gap between HOMO and

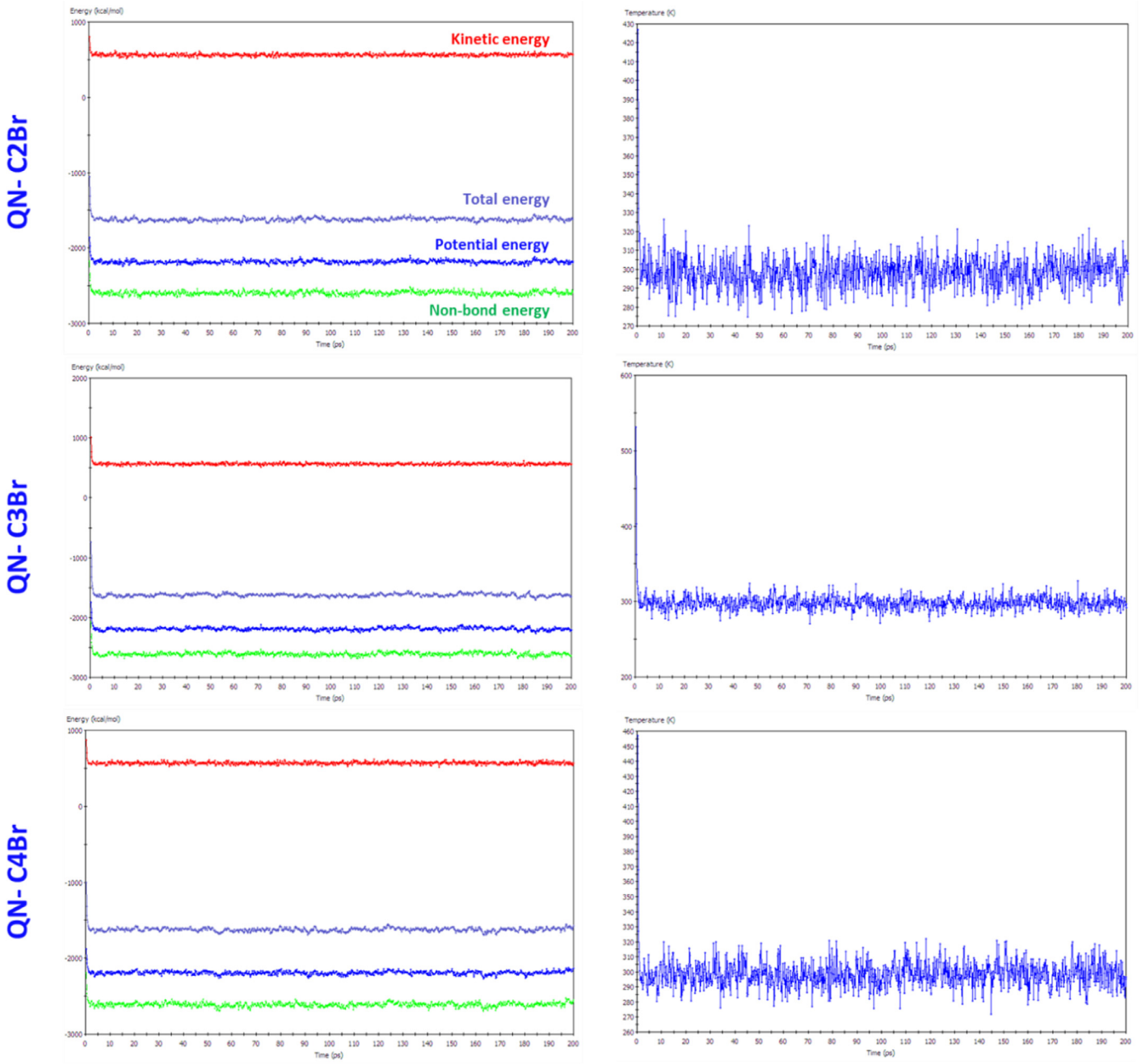

Fig. 17. Energetic and temperature profiles of the studied 8-(n-bromo-R-alkoxy)quinoline + Fe (110) systems during the MD simulations.

LUMO orbitals are closely related parameters each other. The behaviors of inhibitor molecules beside the corrosion of metal surfaces can be illuminated in the light of the numerical values and electronic structure principles regarding to the aforementioned quantities. Chemical hardness [51] is reported as the resistance towards electron cloud polarization or deformation of molecules. According to Pearson, who imparted this concept of science, hard molecules have higher energy gap values and softness is the multiplicative reverse of the hardness. One of the important electronic structure principles in the literature is Maximum Hardness Principle [52] states that "there seems to be a rule of nature that molecules arrange themselves so as to be as hard as possible". According to this principle, chemical hardness is a measure of the stability. Minimum Polarizability Principle [53] state that in a stable state, polarizability is minimized. Soft and polarizable molecules act as good anti-corrosion products. If so, in the brightness of the calculated hardness, softness, energy gap and polarizability values, the anti-corrosion performances of the studied 8-(n-bromo-R-alkoxy)quinoline molecules can be can be offered as QN-C4Br > QN-C3Br > QN-C2Br. Frontier molecular orbital images and energy gaps of the 8-(n-bromo-R-alkoxy)quinoline derivative molecules are given below in Fig. 14.

Electronegativity is a measure electron withdrawal power of chemical species, while the electrophilicity based on absolute hardness and the absolute electronegativity of chemical species reflects electron accepting tendency from electron-rich species of chemical species. Molecules having high electronegativity and electrophilicities exhibit low ant-corrosion efficiency. Within the framework of the data presented, anti-corrosion efficiency classification of the studied 8-(n-bromo-R-alkoxy)quinoline molecules can be given as: QN-C4Br > QN-C3Br > QN-C2Br. This trend is also compatible with experimental observations.

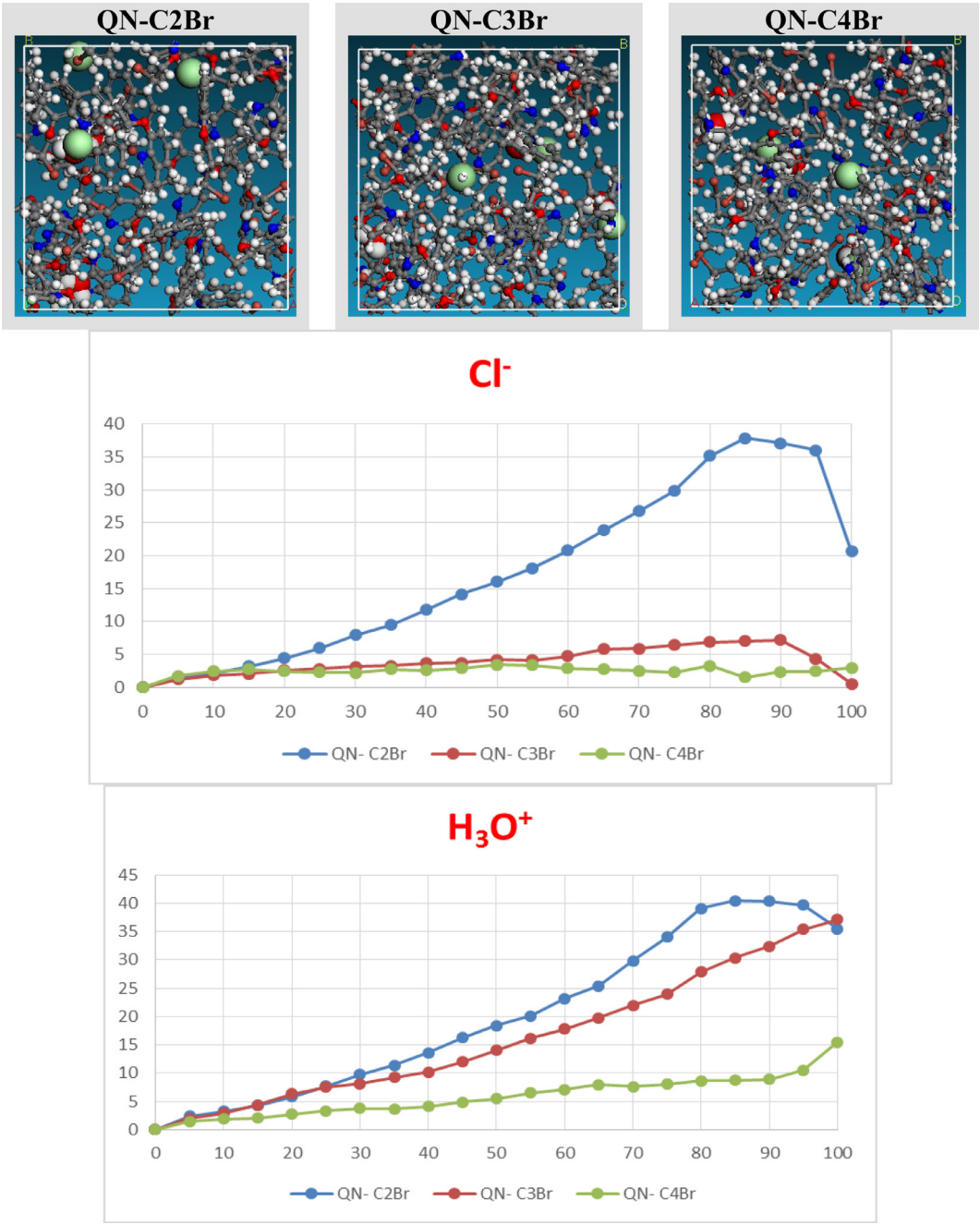

Fig. 18. Used models to calculate "D" coefficient of chosen corrosive species for each inhibitor membrane and their mean squared displacement as a function of the simulation time (100 ps).

However, Gazquez's parameters known as electrodonating and electroaccepting powers provide important hints about electron donating and electron accepting aptitudes of molecules. It is perfect that an effective corrosion inhibitor should easily give the electrons to metal surfaces. The Electroaccepting power value of the QN-C4Br molecule is lower than that of other molecules. This result implies that a QN-C4Br molecule will be more effective against the corrosion of metal surfaces. The fraction of electrons transmitted from inhibitor molecule to the metal surface is an important indicator of anti-corrosion efficiencies of molecules. For $\Delta N>0$, the direction of electron transfer is from inhibitor to metal surface. The higher value of ΔN represents the high corrosion inhibition performance. Back donation energy represents the transfer from the metal surface to inhibitor molecule and this quantity is calculated with the help of global hardness values. The molecules having more negative values of this quantity are not efficacy against the corrosion of metals. Metal-inhibitor interaction energy is one of the useful parameters considered in corrosion inhibition performances. This quantity represents the power of the interaction between inhibitor molecules and metal surfaces. As the metal-inhibitor interaction energy gets negative, corrosion inhibition efficiency increases. Based on the results given in the related table for ΔN, $\Delta\psi$ and $\Delta E_{b\text{-}d}$, anti-corrosion efficiency classification of the studied 8-(n-bromo-R-alkoxy)quinoline molecules can be given as: QN-C4Br > QN-C3Br > QN-C4Br. This performance ranking also is in concordance with experimental results.

On the other hand, Fukui indices are quite important in terms of the analysis of the local reactivity of the studied molecules. In

the following Fig. 15, calculated fukui indices of studied molecules are presented visually. It is important to note that higher values of f^- represent the suitable regions, while a higher value of f^+ corresponds to suitable sites for nucleophilic attack. One can see suitable regions for electrophilic and nucleophilic attack of the studied 8-(n-bromo-R-alkoxy)quinoline molecules from the image presented.

Molecular Dynamics Simulation (MDS) is generally considered to understand the adsorption characteristic of the studied inhibitor molecules and to determine their most stable adsorption configurations on the metal surface [54]. In the light of the calculated adsorption energies, the corrosion inhibition performances of the inhibitor molecules can be easily compared. The calculated adsorption energies of the studied inhibitor molecules are given in Table 7, while the most stable adsorption configurations of the examined inhibitors on Fe (110) surface are presented in Fig. 16. It is apparent from the mentioned figure that inhibitor molecules are positioned in parallel to Fe (110) surface and interact via heteroatoms in their structures with metal surface. In Fig. 17, Energetic and temperature profiles of the studied 8-(n-bromo-R-alkoxy)quinoline derivatives + Fe (110) systems during the MD simulations are represented. Thus, the calculated adsorption energy values for QN-C2Br, QN-C3Br and QN-C4Br are -128.039 kcal mol^{-1}, -135.695 kcal mol^{-1} and -143.822 kcal mol^{-1}, respectively. It is well-known that more negative adsorption energy value belongs to the most effective corrosion inhibitor. According to the adsorption energy values presented, the anti-corrosion efficiency classification can be given as: QN-C4Br > QN-C3Br > QN-C2Br. This classification is compatible with the results of both DFT calculations and experiments made.

Another way for evaluating the corrosion inhibition performances of 8-(n-bromo-R-alkoxy)quinoline derivative molecules is to calculate and use the diffusion coefficient (D) of corrosive species Cl^- and H_3O^+ (Table 8 and Fig. 18). Diffusion ability of corrosive species can be understood from the calculated diffusion coefficient values. It is apparent from the data presented QN-C4Br inhibits the diffusion of corrosive species and protects the MS surface against the corrosion.

4. Conclusions

In this study, three 8-(n-bromo-R-alkoxy)quinoline derivatives with a long hydrocarbon chain have been synthesized and characterized by different spectroscopic technique. These compounds were evaluated for their length chain on the anti-corrosion performance against MS in 1.0 M HCl and the principal important conclusions are:

- QN-C4Br, QN-C3Br and QN-C2Br retard MS corrosion in 1.0 HCl solution with their inhibition efficiency enhanced at increased inhibitor concentrations, and therefore they improve the corrosion resistance of MS in a pickling solution with HCl.
- The potentiodynamic polarization curves indicated that all compounds react as anodic-type inhibitor, and their η_{PP} % depend on the length of the hydrocarbon chain, which confirmed by EIS results.
- The adsorption of corrosion molecule inhibitors QN-C4Br, QN-C3Br and QN-C2Br on MS surface was spontaneous, labeled by electrostatic interactions, and favors the Langmuir adsorption isotherm.
- SEM analysis of the surface indicated the formation of a protective layer on MS surface and the UV-visible spectroscopy of the solution demonstrated the formation inhibitor-complex in solution.
- DFT calculation and MD simulations studies indicated that electrons of aromatic rings, oxygen, and nitrogen heteroatoms, and bromide of 8-(n-bromo-R-alkoxy)quinoline molecules were the major adsorption centers for strong donor/acceptor interactions with the unoccupied d-orbital of MS surface.

Declaration of Competing Interest

The authors declare that they have no known competing financial interests or personal relationships that could have appeared to influence the work reported in this paper.

Acknowledgments

We thank " CAC – Cadi Ayyad University, Marrakech, Morocco" for SEM/EDAX analyses.

References

[1] D. Douche, H. Elmsellem, E.H. Anouar, L. Guo, B. Hafez, B. Tüzün, A. El Louzi, K. Bougrin, K. Karrouchi, B. Himmi, Anti-corrosion performance of 8-hydroxyquinoline derivatives for mild steel in acidic medium: Gravimetric, electrochemical, DFT and molecular dynamics simulation investigations, J. Mol. Liq. 308 (2020) 113042.
[2] B. Hafez, M. Mokhtari, H. Elmsellem, H. Steli, Environmentally friendly inhibitor of the corrosion of mild steel: Commercial oil of Eucalyptus, Int. J. Corros. Scale Inhib. 8 (3) (2019) 573–585.
[3] L.O. Olasunkanmi, M.M. Kabanda, E.E. Ebenso, Quinoxaline derivatives as corrosion inhibitors for mild steel in hydrochloric acid medium: Electrochemical and quantum chemical studies, Physica E 76 (2016) 109–126.
[4] M. Rbaa, A. Oubihi, M. Ouhssine, F. Almalki, T.B. Hadda, A. Zarrouk, B. Lakhrissi, Synthesis of New Heterocyclic Systems Oxazino Derivatives of 8-Hydroxyquinoline: Drug Design and POM Analyses of Substituent Effects on their Potential Antibacterial Properties, Chem. Data Collect. 24 (2019) 100306.
[5] M. Rbaa, S. Jabli, Y. Lakhrissi, M. Ouhssine, F. Almalki, T.B. Hadda, S.M. Moumene, A. Zarrouk, B. Lakhrissi, Synthesis, antibacterial properties and bioinformatics computational analyses of novel 8-hydroxyquinoline derivatives, Heliyon 5 (10) (2019) e02689.
[6] M. Rbaa, A.S. Abousalem, M.E. Touhami, I. Warad, F. Bentiss, B. Lakhrissi, A. Zarrouk, Novel Cu (II) and Zn (II) complexes of 8-hydroxyquinoline derivatives as effective corrosion inhibitors for mild steel in 1.0 M HCl solution: Computer modeling supported experimental studies, J. Mol. Liq. 290 (2019) 111243.
[7] O. Fergachi, F. Benhiba, M. Rbaa, M. Ouakki, M. Galai, R. Touir, M.E. Touhami, Corrosion Inhibition of Ordinary Steel in 5.0 M HCl Medium by Benzimidazole Derivatives: Electrochemical, UV–Visible Spectrometry, and DFT Calculations, J. Bio-and Tribo-Corrosion 5 (1) (2019) 2–13.
[8] S. Indira, G. Vinoth, M. Bharathi, K. Shanmuga Bharathi, Synthesis, spectral, electrochemical, in-vitro antimicrobial and antioxidant activities of bisphenolic mannich base and 8-hydroxyquinoline based mixed ligands and their transition metal complexes, J. Mol. Struct. 1198 (2019) 126886.
[9] M. Rbaa, M. Galai, A.S. Abousalem, B. Lakhrissi, M.E. Touhami, I. Warad, A. Zarrouk, Synthetic, spectroscopic characterization, empirical and theoretical investigations on the corrosion inhibition characteristics of mild steel in molar hydrochloric acid by three novel 8-hydroxyquinoline derivatives, Ionics 13 (8) (2019) 1–20.
[10] S.K. Saha, P. Ghosh, A. Hens, N.C. Murmu, P. Banerjee, Density functional theory and molecular dynamics simulation study on corrosion inhibition performance of mild steel by mercapto-quinoline Schiff base corrosion inhibitor, Physica E 66 (2015) 332–341.
[11] M. Rbaa, B. Lakhrissi, Novel oxazole and imidazole based on 8-Hydroxyquinoline as a Corrosion Inhibition of mild steel in HCl Solution: Insights from Experimental and Computational Studies, Surf. Interfaces 15 (2019) 43–59.
[12] O. Fergachi, F. Benhiba, M. Rbaa, R. Touir, M. Ouakki, M. Galaia, B. Lakhrissi, H. Oudda, M.E. Touhami, Experimental and Theoretical Study of Corrosion Inhibition of Mild Steel in 1.0 M HCl Medium by 2(-4(hloro phenyl-1H-benzo[d]imidazol)-1-yl)phenyl)methanone, Mat. Res. 6 (21) (2018) 1439–1516.
[13] A. Zarrouk, B. Hammouti, A. Dafali, M. Bouachrine, H. Zarrok, S. Boukhris, S.S. Al-Deyab, A theoretical study on the inhibition efficiencies of some quinoxalines as corrosion inhibitors of copperin nitric acid, J. Saudi Chem. Soc. 18 (2014) 450–455.
[14] M. Rbaa, F. Benhiba, I.B. Obot, H. Oudda, I. Warad, B. Lakhrissi, A. Zarrouk, Two new 8-hydroxyquinoline derivatives as an efficient corrosion inhibitors for mild steel in hydrochloric acid: Synthesis, electrochemical, surface morphological, UV–visible and theoretical studies, J. Mol. Liq. 12 (276) (2018) 120–133.
[15] F. El-Hajjaji, M. Messali, M.V. Martínez de Yuso, E. Rodríguez-Castellón, S. Almutairi, Teresa J. Bandosz, M. Algarra, Effect of 1-(3-phenoxypropyl) pyridazin-1-ium bromide on steel corrosion inhibition in acidic medium, J. Colloid Interface Sci. 541 (2019) 418–424.
[16] Y. El Kacimi, H. El Bakri, K. Alaoui, R. Touir, M. Galai, M.Ebn Touhami, M. Doubi, Synergistic effect study of Cetyl Trimethyl Ammonium Bromide with iodide ions at low concentration for mild steel corrosion in 5.0 M HCl medium, Chemical Data Collections 30 (2020) 100558.

[17] D.S. Chauhan, C. Verma, M.A. Quraishi, Molecular structural aspects of organic corrosion inhibitors: Experimental and computational insights, J. Mol. Struct. 1227 (2021) 129374.
[18] L. Lakhrissi, B. Lakhrissi, R. Touir, M.Ebn Touhami, M. Massoui, E.M. Essassi, Mild steel corrosion inhibition in 200 ppm NaCl by new surfactant derivatives of bis-glucobenzimidazolones, Arabian J. Chem. 10 (2017) S3142–S3149.
[19] M. Rbaa, M. Galai, Y. El Kacimi, M. Ouakki, R. Touir, B. Lakhrissi, M.E. Touhami, Adsorption Properties and Inhibition of Carbon Steel Corrosion in a Hydrochloric Solution by 2-(4, 5-diphenyl-4, 5-dihydro-1h-imidazol-2-yl)-5-methoxyphenol, Port. Electrochim. Acta 35 (6) (2017) 323–338.
[20] Y. El Kacimi, H. ElBakri, R.Touir K.Alaoui, M. Galai, M. EbnTouhami, M Doubi, Synergistic effect study of Cetyl Trimethyl Ammonium Bromide with iodide ions at low concentration for mild steel corrosion in 5.0 M HCl medium, Chemical Data Collections 30 (December 2020) 100558.
[21] M. Doubi, S. Abbout, H. Erramli, A. Dermaj, D. Cchebabe, R. Touir, N. Hejjaji, Performance of the novel corrosion inhibitor based on Cetamine to protect mild steel in surface water solution: electrochemical and surface studies, Chem. Pap. (2020), doi:10.1007/s11696-020-01413-w.
[22] N. Islam, S. Kaya, Conceptual density functional theory and its application in the chemical domain, CRC Press, 2018.
[23] S. Kaya, C. Kaya, A new method for calculation of molecular hardness: a theoretical study, Computational and Theoretical Chemistry 1060 (2015) 66–70.
[24] R.G. Parr, L.V. Szentpály, S. Liu, Electrophilicity index, J. Am. Chem. Soc. 121 (9) (1999) 1922–1924.
[25] P.K. Chattaraj, D.R. Roy, Update 1 of: electrophilicity index, Chem. Rev. 107 (9) (2007) PR46–PR74.
[26] C. Morell, J.L. Gázquez, A. Vela, F. Guégan, H. Chermette, Revisiting electroaccepting and electrodonating powers: proposals for local electrophilicity and local nucleophilicity descriptors, PCCP 16 (48) (2014) 26832–26842.
[27] T. Koopmans, Über die Zuordnung von Wellenfunktionen und Eigenwerten zu den einzelnen Elektronen eines Atoms, Physica 1 (1–6) (1934) 104–113.
[28] Ş. Erdoğan, Z.S. Safi, S. Kaya, D.Ö. Işın, L. Guo, C. Kaya, A computational study on corrosion inhibition performances of novel quinoline derivatives against the corrosion of iron, J. Mol. Struct. 1134 (2017) 751–761.
[29] L. Guo, S. Kaya, I.B. Obot, X. Zheng, Y. Qiang, Toward understanding the anticorrosive mechanism of some thiourea derivatives for carbon steel corrosion: A combined DFT and molecular dynamics investigation, J. Colloid Interface Sci. 506 (2017) 478–485.
[30] Y. Yan, X. Wang, Y. Zhang, P. Wang, X. Cao, J. Zhang, Molecular dynamics simulation of corrosive species diffusion in imidazoline inhibitor films with different alkyl chain length, Corros. Sci. 73 (2013) 123–129.
[31] M. Khattabi, F. Benhiba, S. Tabti, A. Djedouani, A. El Assyry, R. Touzani, I. Warad, H. Oudda, A. Zarrouk, Performance and computational studies of two soluble pyran derivatives as corrosion inhibitors for mild steel in HCl, J. Mol. Struct. 1196 (2019) 231–244.
[32] Y. El Kacimi, H. El Bakri, K. Alaoui, R. Touir, M. Galai, M Ebn Touhami, M. Doubi, Synergistic effect study of Cetyl Trimethyl Ammonium Bromide with iodide ions at low concentration for mild steel corrosion in 5.0 M HCl medium, Chemical Data Collections 30 (2020) 100558.
[33] J. Cruz, T. Pandiyan, E. Garcia-Ochoa, J. Electroanal. Chem. 583 (2005) 8–16.
[34] D.S. Chauhan, C. Verma, M.A. Quraishi, Molecular structural aspects of organic corrosion inhibitors: Experimental and computational insights, J. Mol. Struct. 1227 (2021) 129374.
[35] R. Khrifou, R. Touir, A. Koulou, H. ElBakri, M. Rbaa, M. EbnTouhami, A. Zarrouk, F. Benhiba, The influence of low concentration of 2-(5-methyl-2-nitro-1H-imidazol-1-yl)ethyl benzoate on corrosion brass in 0.5 M H2SO4 solution, Surf. Interfaces 24 (2021) 101088.
[36] S. Attabi, M. Mokhtari, Y. Taibi, I. Abdel Rahman, B. Hafez, H. Elmsellem, Electrochemical and Tribological Behavior of Surface-Treated Titanium Alloy Ti–6Al–4V, Journal of Bio- and Tribo-Corrosion (2019) 2 5.
[37] I.B. Obot, N.O. Obi-Egbedi, N.W. Odozi, Acenaphtho [1,2-b] quinoxaline as a novel corrosion inhibitor for mild steel in 0.5M H2SO4, Corros. Sci. 52 (2010) 923–926.
[39] S.S. El-Rehim, M.A.M. Ibrahim, K.F. Khaled, 4-Aminoantipyrine as an inhibitor of mild steel corrosion in HCl solution, J. Appl. Electrochem. 29 (1999) 593.
[38] A. Yuce, G. Kardas, Adsorption and inhibition effect of 2-thiohydantoin on mild steel corrosion in 0.1 M HCl, Corros. Sci. 58 (2012) 86–94.
[40] A. Popova, M. Christov, Corros. Sci. 48 (2006) 3208–3221.
[41] N. Errahmany, M. Rbaa, A.S. Abousalem, A. Tazouti, M. Galai, E.H. El Kafssaoui, M.Ebn Touhami, B. Lakhrissi, R. Touir, Experimental, DFT calculations and MC Simulation s Concept of novel quinazolinone derivatives as Corrosion Inhibitor for Mild Steel in 1.0 M HCl medium, J. Mol. Liq. (2020), doi:10.1016/j.molliq.2020.113413.
[42] Y. El Aoufir, R. Aslam, F. Lazrak, R. Marzouki, S. Kaya, S. Skal, I.M. Chung, The effect of the alkyl chain length on corrosion inhibition performances of 1, 2, 4-triazole-based compounds for mild steel in 1.0 M HCl: Insights from experimental and theoretical studies, J. Mol. Liq 303 (2020) 112631.
[43] H. Jafari, K. Akbarzade, I. Danaee, Corrosion inhibition of carbon steel immersed in a 1 M HCl solution using benzothiazole derivatives, Arab. J. Chem 12 (7) (2019) 1387–1394.
[44] O. Fergachi, F. Benhiba, M. Rbaa, M. Ouakki, M. Galai, R. Touir, B. Lakhrissi, H. Oudda, M.Ebn Touhami, Corrosion Inhibition of Ordinary Steel in 5.0 M HCl Medium by Benzimidazole Derivatives: Electrochemical, UV–Visible Spectrometry, and DFT Calculations, Journal of Bio- and Tribo-Corrosion 5 (2019), doi:10.1007/s40735-018-0215-3.
[45] K. Alaoui, R. Touir, M. Galai, H. Serrar, M. Ouakki, S. Kaya, B. Tüzün, S. Boukhris, M.Ebn Touhami, Y. El Kacimi, Electrochemical and Computational Studies of Some Triazepine Carboxylate Compounds as Acid Corrosion Inhibitors for Mild Steel, J. Bio- and Tribo-Corrosion 4 (2018), doi:10.1007/s40735-018-0154-z.
[46] S.A. Ali, M. A., R.F.Al-Ghamdi E-Shareef, M.T. Saeed, The isoxazolidines: the effects of steric factor and hydrophobic chain length on the corrosion inhibition of mild steel in acidic medium, Corros. Sci. 47 (11) (2005) 2659–2678.
[47] H. Hamani, T. Douadi, M. Al-Noaimi, S. Issaadi, D. Daoud, S. Chafaa, Electrochemical and quantum chemical studies of some azomethine compounds as corrosion inhibitors for mild steel in 1 M hydrochloric acid, Corros. Sci. 88 (2014) 234–245.
[48] A. Yousefi, S.A. Aslanzadeh, J. Akbari, Experimental and DFT studies of 1-methylimidazolium trinitrophenoxide as modifier for corrosion inhibition of SDS for mild steel in hydrochloric acid, Anti-Corros. Methods Mater. 65 (1) (2018) 107–122.
[49] M. El Faydy, R. Touir, M.Ebn Touhami, A. Zarrouk, C. Jama, B. Lakhrissi, L.O. Olasunkanmi, E.E. Ebenso, F. Bentiss, Corrosion inhibition performance of newly synthesized 5-alkoxymethyl-8-hydroxyquinoline derivatives for carbon steel in 1 M HCl solution: experimental, DFT and Monte Carlo simulation studies, Phys. Chem. Chem. Phys. 20 (2018) 20167.
[50] M. Rbaa, M. Fardioui, C. Verma, A.S. Abousalem, M. Galai, T.Guedira Ebenso, B. Lakhrissi, I. Warad, A. Zarrouk, 8-Hydroxyquinoline based chitosan derived carbohydrate polymer as biodegradable and sustainable acid corrosion inhibitor for mild steel: Experimental and computational analyses, Int. J. Biol. Macromol. 155 (2020) 645–655.
[51] S. Kaya, C. Kaya, A new equation for calculation of chemical hardness of groups and molecules, Mol. Phys. 113 (11) (2015) 1311–1319.
[52] S. Kaya, C. Kaya, A simple method for the calculation of lattice energies of inorganic ionic crystals based on the chemical hardness, Inorg. Chem. 54 (17) (2015) 8207–8213.
[53] P.K. Chattaraj, S. Sengupta, Popular electronic structure principles in a dynamical context, J. Phys. Chem. 100 (40) (1996) 16126–16130.
[54] L. Guo, I.B. Obot, X. Zheng, X. Shen, Y. Qiang, S. Kaya, C. Kaya, Theoretical insight into an empirical rule about organic corrosion inhibitors containing nitrogen, oxygen, and sulfur atoms, Appl. Surf. Sci. 406 (2017) 301–306.

Filters Clear All

- *Web of Science* Coverage
- Open Access
- Category
- Country / Region
- Language
- Frequency
- Journal Citation Reports

Refine Your Search Results

JOURNAL OF MOLECULAR STRUCTURE Search

Sort By: Relevancy

Search Results

Found 948 results (Page 1) Share These Results

Exact Match Found

JOURNAL OF MOLECULAR STRUCTURE

Publisher: **ELSEVIER , RADARWEG 29, AMSTERDAM, NETHERLANDS, 1043 NX**
ISSN / eISSN: **0022-2860 / 1872-8014**
Web of Science Core Collection: **Science Citation Index Expanded**
Additional *Web of Science* Indexes: **Current Contents Physical, Chemical & Earth Sciences | Essential Science Indicators**

Share This Journal View profile page

Other Possible Matches

NATURE STRUCTURAL & MOLECULAR BIOLOGY

Publisher: **NATURE PORTFOLIO , HEIDELBERGER PLATZ 3, BERLIN, Germany, 14197**
ISSN / eISSN: **1545-9993 / 1545-9985**
Web of Science Core Collection: **Science Citation Index Expanded**
Additional *Web of Science* Indexes: **Biological Abstracts | BIOSIS Previews | Current Contents Life Sciences | Essential Science Indicators**

Share This Journal View profile page

ALGORITHMS FOR MOLECULAR BIOLOGY

OPEN ACCESS

Publisher: **BMC , CAMPUS, 4 CRINAN ST, LONDON, ENGLAND, N1 9XW**
ISSN / eISSN: **1748-7188**

Results: 1
(from Web of Science Core Collection)

You searched for: TITLE: (Effect of hydrocarbon chain length for acid corrosion inhibition of mild steel by three 8-(n-bromo-R-alkoxy)quinoline derivatives: Experimental and theoretical investigations) ...More

Create an alert

Refine Results

Search within results for...

Publication Years
- 2021 (1)

Refine

Web of Science Categories
- CHEMISTRY PHYSICAL (1)

Refine

Document Types
- ARTICLE (1)

Refine

Organizations-Enhanced
- CUMHURIYET UNIVERSITY (1)
- IBN TOFAIL UNIVERSITY OF KENITRA (1)
- IBN ZOHR UNIVERSITY OF AGADIR (1)
- MOHAMMED V UNIVERSITY IN RABAT (1)
- REG CTR EDUC TRAINING PROFESS CRMEF (1)

more options / values...

Refine

Funding Agencies

Authors

Source Titles

View all options

For advanced refine options, use
Analyze Results

Sort by: Date Times Cited Usage Count Relevance More

1 of 1

Select Page Export... Add to Marked List

Analyze Results
Create Citation Report

1. **Effect of hydrocarbon chain length for acid corrosion inhibition of mild steel by three 8-(n-bromo-R-alkoxy)quinoline derivatives: Experimental and theoretical investigations**

By: Tazouti, A.; Errahmany, N.; Rbaa, M.; et al.

JOURNAL OF MOLECULAR STRUCTURE Volume: 1244 Article Number: 130976 Published: NOV 15 2021

View Abstract

Times Cited: 1
(from Web of Science Core Collection)

Usage Count

Select Page Export... Add to Marked List

Sort by: Date Times Cited Usage Count Relevance

Show: 10 per page

1 records matched your query of the 78,725,508 in the data limits you s

JOURNAL OF MOLECULAR STRUCTURE

Impact Factor

3.196	2.618
2020	*5 year*

JCR® Category	*Rank in Category*	*Quartile in Category*
CHEMISTRY, PHYSICAL	83 of 162	Q3

Data from the 2020 edition of Journal Citation Reports

Publisher
ELSEVIER, RADARWEG 29, 1043 NX AMSTERDAM, NETHERLANDS

ISSN: 0022-2860
eISSN: 1872-8014

Research Domain
Chemistry

Close Window